Nanozyme: new horizons for responsive biomedical applications

Dawei Jiang[a,b], **Dalong Ni**[a], **Zachary T. Rosenkrans**[a], **Peng Huang**[b], **Xiyun Yan**[c], **Weibo Cai**[a]

[a]Departments of Radiology, Medical Physics, and Pharmaceutical Sciences, University of Wisconsin – Madison, Madison, WI, 53705, USA

[b]Marshall Laboratory of Biomedical Engineering, International Cancer Center, Laboratory of Evolutionary Theranostics (LET), School of Biomedical Engineering, Shenzhen University Health Science Center, Shenzhen, 518060, China

[c]Key Laboratory of Protein and Peptide Pharmaceuticals, Institute of Biophysics, Chinese Academy of Sciences, Beijing, 100049, China

Abstract

Nanozymes are nanomaterial-based artificial enzymes. By effectively mimicking catalytic sites of natural enzymes or harboring multivalent elements for reactions, nanozyme systems have successfully served as direct surrogates of traditional enzymes for catalysis. With the rapid development and ever-deepening understanding of nanotechnology, nanozymes offer higher catalytic stability, ease of modification and lower manufacturing cost than protein enzymes. Additionally, nanozymes possess inherent nanomaterial properties, providing not only a simple substitute of enzymes but also a multimodal platform interfacing complex biologic environments. Recent extensive research has focused on designing various nanozyme systems that are responsive to one or multiple substrates by tailored means. Catalytic activities of nanozymes can be regulated by pH, H_2O_2 and glutathione concentrations and levels of oxygenation in different microenvironments. Moreover, nanozymes can be remotely-controlled *via* different stimuli, including a magnetic field, light, ultrasound, and heat. Collectively, these factors can be adjusted to maximize the diagnostic and therapeutic efficacies of different diseases in biomedical settings. Therefore, by integrating the catalytic property and inherent nanomaterial nature of nanozyme systems, we anticipate that stimuli-responsive nanozymes will open up new horizons for diagnosis, treatment, and theranostics.

1 Introduction

Nanozyme, the umbrella term for an emerging paradigm, encompasses a large number of artificial nanomaterials with intrinsic enzyme-like activities.[1,2] Since natural enzymes are mostly globular proteins (a few others are RNA ribozymes), they are generally costly to manufacture and store, unstable to transfer or modify, and sensitive to harsh physiochemical conditions. After systematic investigation of the structure–function relationships of natural

wcai@uwhealth.org; peng.huang@szu.edu.cn; yanxy@ibp.ac.cn.

enzymes, researchers hypothesized that rational assembly of functional atoms or molecules might produce similar catalytic activities toward enzyme substrates and present a self-assembled enzyme-mimicking system.[3] Recent advances in nanotechnology have spawned new developments in this direction and empowered scientists with an ever-evolving toolbox of artificial enzymes. Among them, the nanozyme concept has revolutionized our fundamental understanding of biology and chemistry, facilitating a plethora of applications in the fields of biosensing, biology, and medicine.

In 2004, Scrimin and co-workers coined the term "nanozyme" and applied triazacyclonane-functionalized gold nanoparticles as catalysts for transphosphorylation reaction.[3] After anchoring triazacyclonane on the surface of gold nanoparticles for Zn^{2+} ion chelation, this nanozyme can be used for the cleavage of phosphate esters. The design of this nanozyme highlights the concept of cooperativity among Zn^{2+} ions on the gold nanoparticle surface and inspired researchers in this emerging field. Later in 2007, we reported the intrinsic peroxidase-like activity of magnetic nanoparticles (Fe_3O_4).[4] As an alternative method of preparing a nanozyme system, our discovery utilized a single element with different valences for catalytic reactions. Emerging studies have since unveiled that various metal and metal oxide nanoparticles (such as iron oxide, ceria, and gold nanoparticles), carbon nanomaterials (including carbon nanotubes and graphene oxide) and multiple metal–organic frameworks (MOFs) exhibit excellent catalytic activities by mimicking natural enzymes' structures or functions.[5,6] Collectively, these nanozyme systems offer higher catalytic stability, ease of modification and lower manufacturing cost in various biomedical applications when compared with natural enzymes.

A variety of archetypal nanozyme systems have been reported and comprehensively reviewed in the literature.[1,2,5–7] However, few works have been devoted to discussing the classification of nanozymes with regard of their mode of action toward one or more substrates and the cooperative design of nanozymes for biomedical applications. To highlight the importance of nanozymes in the fields of chemistry, biology, and medicine, this review discusses research efforts on tailored nanozyme systems responsive to one or multiple substrates. We also review the latest biomedical applications of nanozymes categorized into three subtypes based on their mode of application, including self-acting, synergistic, and remotely-controlled nanozymes. We further present how nanozymes enable advances in biomedicine and demonstrate the underlying design strategies to improve the diagnostic and therapeutic efficacy for different diseases. Finally, we discuss current challenges and future directions of nanozyme development with a view to maximizing their great potential. Due to the space limitations, we only discuss nanozymes that present inherent enzyme activities but not nanosystems loaded with natural enzymes. Readers are thus referred to research and review articles for more information regarding other catalytic nanosystems beside nanozymes (Scheme 1).

2 Nanozymes with a single-substrate mechanism

Nanozymes that only react with a single substrate will be introduced in this section within a paradigm to demonstrate the basic design principles and catalytic mechanisms of nanozymes. Various nanozymes have been reported with enzyme-mimicking activity while

providing rigid yet water-soluble platforms. Essential functional groups are cooperatively anchored on various nanoscale platforms for catalytic reactions. Later, nanozymes homing multivalent elements (metal ions or carbon atoms) were discovered and have found an increasing number of applications in biomedical fields. The most representative nanozymes with single-substrate mechanisms will be categorized into several subtypes based on their reactions and the types of natural enzymes they mimic.

Nanozymes with a single-substrate mechanism generally exhibit a Michaelis-Menten catalytic kinetic profile, where the catalysis has both the binding and reaction phases (Scheme 2). When plotting the reaction velocity as a function of substrate concentration, k_{cat} (maximal reaction rate) and K_M (substrate concentration where reaction rate reaches half of the maximal) are typically calculated to define the nanozyme activity. During the initial stage of the activity curve, the reaction curve rises linearly so that the slope (k_{cat}/K_M) can also be used to describe the nanozyme activity (Scheme 2).

2.1 Hydrolase

Phosphodiesterase (PDE) catalyzes the hydrolysis of phosphodiester bonds. In biological systems, PDE is mainly responsible for the cleavage of phosphate bonds of cyclic 3,5 adenosine monophosphate (cAMP) and cyclic 3,5 guanosine monophosphate (cGMP). By degrading both cAMP and cGMP, PDE plays an essential role in regulating the intensity, localization, and duration of cyclic nucleotide signaling within subcellular organelles. The hydrolysis of phosphodiester bonds requires the cooperation of multiple metal ion centers from PDEs and H-bond (electron) donors from the substrate molecules.

To mimic the function of PDEs using nanozymes, Scrimin and co-workers anchored triazacyclononane units on the surface of gold nanoparticles (AuNPs) to home Zn^{2+} ions as metal ion centers needed for phosphodiester hydrolysis.[3] With 2-hydroxypropyl p-nitro-phenyl phosphate (HPPNP) as a test substrate, the peak activity for the AuNP nanozyme occurred when Zn^{2+} was fully loaded (Fig. 1A). Kinetic profiling suggested a single-substrate mechanism with the apparent Michaelis–Menten parameters $K_M = 0.93$ mM and $k_{cat} = 4.2 \times 10^{-3}$ s^{-1}. When compared with free Zn^{2+} chelated triazacyclononane molecules, the significantly improved catalytic activity of the nanozyme suggested high cooperativity of Zn^{2+} ions anchored in close proximity on the surface of AuNPs. Later, this AuNP nanozyme was presented with biologically-relevant RNA samples, namely UpU, ApA and CpC RNA dinucleotides. The nanozyme was most active with UpU and fairly active toward ApA and CpC. It was later found that the stability of di-anionic transition state of AuNP nanozymes in aqueous solution plays central role in accelerating the reaction.[8] The advantage of nanozymes emerged when the reactivity was compared to the existing benchmark molecule for HPPNP cleavage in water (Fig. 1B). The polarity of the AuNP surface was decreased by extending the carbon chain spacers, which improved nanozyme stability in the transition state and produced a more than 10-fold increase in k_{cat}. The reactivity increase resulted from improved cooperativity between metal ions and H-bond donors, an expected result from the rational design of the nanozyme platform.

Phosphotriesterase (PTE) is a protein enzyme containing metal ion centers for hydrolysis of tri-ester bonds. The active sites were found to be Zn–OH–Zn, which could be easily

replicated using MOFs (Fig. 1C).[5] Farha, Hupp, and co-workers screened multiple MOFs as artificial phosphotriesterases, which could find broad application in denaturing of chemical warfare agents, such as nerve agents and their simulants.[9] Zr_6-containing NU-1000 with a big pore size (3.1 nm) was able to accelerate the hydrolysis of a nerve agent simulant dimethyl 4-nitrophenyl phosphate (DMNP) and GD (also known as Soman) as shown in Fig. 1D. The Zr–OH–Zr moieties in the NU-1000 MOF well replicated the Zn–OH–Zn catalytic sites in the natural enzyme.

2.2 Peroxidase

Peroxidases encompass a large group of enzymes that catalyze the oxidation of substrates in the presence of peroxides (mostly H_2O_2 with a few as organic hydroperoxides). Substrates normally serve as electron donors and the reaction is shown in Fig. 2A. In 2007, Yan and colleagues first unveiled the hidden property of Fe_3O_4 magnetic nanoparticles (MNPs) as potent intrinsic peroxidases.[4] They tested Fe_3O_4 MNPs with three sizes (30, 150, and 300 nm) and found that they all catalyzed the oxidation of 3,3,5,5-tetramethylbenzidine (TMB) with H_2O_2. Fe_3O_4 MNPs also oxidized some other molecules (DAB and OPD), mimicking the enzyme activity of horseradish peroxidase (HRP). The catalytic activity of Fe_3O_4 MNPs was found to be dependent on pH, temperature, H_2O_2 concentration and size. When compared with HRP, Fe_3O_4 MNP showed peroxidase activity in a larger pH range (0–12) with improved temperature tolerance (4–90 °C) and faster reaction rates. This makes Fe_3O_4 MNP nanozymes robust substitutes of natural peroxidases. Detailed investigation of the mode of action suggested a ping pong mechanism similar to HRP, where one product is released before another substrate molecule binds the enzyme/nanozyme. In the case of MNPs, they bind H_2O_2 and transfer electrons from substrate molecules to generate oxidized products and water. Since Fe^{2+} and Fe^{3+} both exist on MNPs, this nanozyme may maintain catalytic activity in the presence of excessive H_2O_2 or other oxidants, presenting a wider functional range than HRP or other enzymes.

This work has inspired many other types of peroxidase-like nanozymes with redox metal ion couples and enabled a broad range of applications in chemical assay and biomedicine. Iron chalcogenides (FeS nanosheets, FeSe nanoparticles), iron phosphates, doped ferrites (such as $CoFe_2O_4$ and $BiFeO_3$), metal-based nanoparticles (Au, and Au@Pt nanomaterials), and many metal oxide/chalcogenide nanomaterials (CuO, Co_3O_4, CdS and so on) were found to be peroxidase-mimicking. Almost all these nanoparticles have large surface area to volume ratios, enhanced binding capacities relative to protein-based enzymes, and high affinity to H_2O_2, facilitating the binding of substrates and subsequent electron transfer.[2]

In 2010, Qu and co-workers identified the peroxidase-like activity of single-walled carbon nanotube (SWCN) and graphene oxide (GO).[10] The carbon nanomaterials themselves, without the presence of metal ions, catalyzed the TMB blue color reaction upon addition of H_2O_2 at pH 4.0, a similar working condition required by HRP. These carbon-based nanozyme reactions can both be saturated by excessive H_2O_2 or quenched by the addition of H_2SO_4, resembling reactions using natural HRP. High surface area to volume ratio and enhanced absorption of substrates both contributed to the catalytic activities of SWCN and GO. The binding of SWNT and GO to H_2O_2 were slower than HRP. Yet, the K_M values of

SWNT and GO to TMB indicated that the reaction rates were in fact more than 10-fold faster than HRP. Further studies suggested a ping pong mechanism, where TMB or other substrate molecules are absorbed to carbon nanozymes to facilitate the transfer of highly enriched electrons from substrates to hydrogen peroxide.

Natural vanadium haloperoxidase (V-HPOs) has been used as additives in antifouling coatings to prevent the formation of biofilm on the surface of sea products. However, scaling up the production of V-HPOs has always been costly and their stability and reactivity remain limited under seawater conditions (pH 8.3). In 2012, Tremel reported that vanadium pentoxide (V_2O_5) nanowires can mimic V-HPOs and convert bromide, in the presence of H_2O_2, into water and HOBr (Fig. 2B).[11] The K_M values were estimated to be 10 μM for H_2O_2 and 0.2 mM for bromide and the k_{cat} was approximately 7.3×10^{-6} s^{-1}. Later in 2014, Mugesh and co-workers found that V_2O_5 nanowires also catalyze glutathione (GSH) to glutathione disulfide in a glutathione peroxidase (GPx) manner.[12] V_2O_5 nanowires were tested with glutathione reductase (GR) to enable recycling of glutathione disulfide back to GSH (Fig. 2C). No antioxidant activity from the V_2O_5 nanozyme was detected when incubated with GSH and GR, confirming the enzyme-mimicking activity is specific to V_2O_5. A typical Michaelis-Menten reaction kinetic was observed and K_M values were found to be 0.11 mM for H_2O_2 and 2.22 mM for GSH, with a k_{cat} value of 0.065 s^{-1}.

Recently, MOFs have drawn much attention as another type of peroxidase-mimicking nanozyme, which serves as an excellent model to validate our understanding of how nanozymes and their catalytic reactions function.[5] The active sites of natural peroxidases normally involve a multivalent metal ion (Fe^{2+}/Fe^{3+}, Cu^{1+}/Cu^{2+}) that initiates the reaction. Nanozymes, especially MOFs, may anchor multiple redox couples and make them active reaction sites for catalysis. This may enable the mimicking of peroxidase activities given rational design for better cooperativity between redox couples and substrate molecules. By chelating metal ions (normally Fe and Cu) with organic ligands, catalytic sites could be created to achieve optimal cooperativity for peroxidase reactions (Fig. 2A).[5] A Fenton-like mechanism is suggested where H_2O_2 is first absorbed to the MOF surface and the O–O bond breaks down to produce $^{\bullet}$OH radicals. Electron spin resonance (ESR) spectroscopy identified the existence of hydroxyl radicals during the enzyme reaction using MOF in the presence of H_2O_2. To maximize the reaction efficiency, ultrathin 2D MOF nanosheets were preferred over 3D bulk MOF analogues due to the highly exposed surface areas and increased binding sites for enzymatic catalysis.[13,14] Peroxidase-like MOF nanozymes excellently illustrate how artificial nanomaterials may mimic the function of peroxidases by harboring the most essential parts of natural enzymes.

2.3 Superoxide dismutase

Superoxide dismutase (SOD) disproportionates superoxide radicals into oxygen and hydrogen peroxide and alleviates oxidative stress generated from cell metabolism (Fig. 3A). A multivalent metal ion, such as $Cu^{1+/2+}$, $Mn^{2+/3+}$, $Fe^{2+/3+}$ and $Ni^{2+/3+}$, is required for the reaction to proceed. For example, McGinnis and co-workers found that cerium oxide nanoparticles (nanoceria) may serve as oxygen buffers and act as SOD to scavenge superoxide radicals generated by radiotherapy. Nanoceria was found to protect cellular

damage and retinal degeneration caused by radiation or light generated superoxide radicals and other reactive oxygen species (ROS).[15]

Fullerene and its derivatives have long been established as free radical "sponges" due to their excellent ability to scavenge various types of ROS. They have been reported to protect the brain from neuron damage produced by over-generated superoxide radicals. In 2004, Ali *et al.* investigated the interaction of C_3 tris malonyl-C_{60} derivative (C_3-fullerene) with superoxide radicals and demonstrated the SOD-mimetic activity of C_3-fullerene (Fig. 3B).[16] The study ruled out the possibility of C_3-fullerene stoichiometrically scavenging superoxide radicals *via* straightforward redox reactions and proved the reaction to be catalytic dismutation. This conclusion was corroborated by the unvarying concentration of C_3-fullerene after exposure to additional superoxide radicals. The reaction also produced hydrogen peroxide and oxygen. Together, these observations established fullerene as a SOD mimic. Profiling on the kinetics showed that the catalysis was carried out through a ping pong mechanism: C_3-fullerene first accepts an electron pair from one superoxide radical and transfer the electron pair to another superoxide radical. The first step generates oxygen and is the rate-determining step. The catalytic rate constant was measured to be $2.2\ (\pm 0.1) \times 10^6$ $M^{-1}\ s^{-1}$ at pH 7.4. The pH decrease results in more carboxyl groups present on the surface of fullerene, constituting a thicker electrostatic barrier to superoxide radicals and suppress the catalytic activity.

In 2015, Tour and co-workers reported the SOD-like activity of hydrophilic carbon clusters (HCCs), obtained from oxidation of single-walled carbon nanotubes with nitric acid and sulfuric acid.[17] After PEGylation, the planar PEG-HCC was found to transform superoxide radicals into oxygen and H_2O_2. Mechanism studies indicated that PEG-HCC converted two superoxide radicals into one hydrogen peroxide, one oxygen, and two hydroxide radicals. The k_{cat} value for PEG-HCC was found to be $1.05 \times 10^6\ s^{-1}$, comparable to Cu/Zn SOD under a similar condition ($0.65 \times 10^6\ s^{-1}$). The catalysis is specific to superoxide radicals ($O_2^{\bullet-}$) but remains inert to nitric oxide ($NO^{\bullet}$) or peroxynitrite ($ONOO^-$) radicals, making PEG-HCC a selective SOD-mimicking nanozyme.

2.4   Oxidase

Natural oxidase catalyzes the oxidation of substrates using oxygen as the electron acceptor. Subsequently, O_2 is reduced to water or hydrogen peroxide. In 2004, Rossi and co-workers reported the oxidase-mimicking activity of naked gold nanoparticles.[20] D-glucose was selectively oxidized to D-gluconic acid without any production of a fructose isomer. Kinetic measurement indicated that the catalytic rate constant was approximately $3.0 \times 10^6\ M^{-1}\ s^{-1}$. The gold nanoparticle first absorbed a hydrated glucose molecule on the surface, which then attacked a dissolved oxygen in a nucleophilic way and generated one gluconic acid and one hydrogen peroxide. Other metal nanoparticles of similar size (3–5 nm) showed no evidence of oxidase-mimicking activity, including Cu, Ag, Pd and Pt. Catalysis is eradicated by aggregation of gold nanoparticles or the presence of sulfur compounds. Thus, reducing the size of gold nanoparticles increased the oxidation efficiency. Additionally, when supported with mesoporous carbon to hamper aggregation, gold nanoparticles presented improved catalytic activities.

Sulfite oxidase contains molybdenum and catalyzes sulfite to sulfate in amino acids and lipid metabolism. In 2014, Tremel and co-workers found that molybdenum trioxide nanoparticles (~2 nm) have intrinsic sulfite oxidase activity.[18] They were found to target mitochondria on the cellular level when functionalized with triphenylphosphonium ions and detoxify sulfite in the absence of sulfite oxidase. Electron paramagnetic resonance (EPR) spectroscopy detected a Mo^{5+} intermediate in the natural sulfite oxidase but not the MoO_3 nanozyme. Steady-state kinetics studies of the MoO_3 nanozyme suggested that it first accepted two electrons from sulfite that reduced Mo^{4+} to Mo^{6+} in the presence of $[Fe(CN)_6]^{3-}$ (Fig. 3C). The K_M value for sulfite is 0.59 ± 0.02 mM and k_{cat} is 2.78 ± 0.09 s^{-1}, indicating that the MoO_3 nanozyme was slightly more efficient than native human sulfite oxidase.

In 2015, Lercher and co-workers found that Cu-exchanged zeolites (microporous aluminosilicate minerals) with a mordenite structure may actively mimic the function of methane monooxygenase and oxidize methane to methanol (Fig. 3D).[19] Cu and Fe are two major elements found in active sites of methane monooxygenase. Zeolite mordenite has a 12-membered ring that can be used to stabilize $[Cu_3(\mu-O)_3]^{2+}$ complex for oxidation. The methane molecules may first attack the Cu-oxide complex to produce $CH_3^{\bullet}$ and a Cu-bound OH group. Then, methanol is formed with two neighboring Cu-oxide complexes. Iron-containing zeolites have similar effects of oxidizing methane to methanol after their activation by N_2O.[21]

2.5 Catalase and others

Catalase accelerates the dismutation of H_2O_2 into water and oxygen (Fig. 3A). Many nanozymes, such as metal, metal oxides and Prussian Blue nanoparticles, with peroxidase or SOD-like activities also present catalase-mimicking properties. These nanozyme systems generally have high affinities for hydrogen peroxide and other ROS radicals. At certain pH or temperature, nanozyme systems can accelerate the dismutation of surface-bound H_2O_2 over their other enzyme-mimicking activities.[2] Several representative nanozymes that can mimic multiple enzymes will be discussed in the next section.

3 Nanozymes with a multi-substrate mechanism

As the development of nanotechnology and the understanding of artificial enzymes have amassed, nanozymes and their mechanisms of multiple enzyme-like activities have been identified. In this section, we list representative nanozymes that act on more than one substrate or act differently under distinct environments, including different pH values, glutathione or hydrogen peroxide concentrations, as well as levels of oxygenation. These factors may significantly influence the behaviors of nanozymes, which is especially true for the biological microenvironment at disease sites such as cancer.

3.1 Metal-based nanozymes

Many noble metal-based nanoparticles present pH-dependent peroxidase and catalase-mimicking properties, such as gold, silver, palladium, platinum nanoparticles and their hybrids (Fig. 4A).[22] At lower pH, they present peroxidase-like activity and catalyze H_2O_2 into $^{\bullet}OH$ radicals; at higher pH, they are catalase-mimicking and generate oxygen from

H_2O_2. The pH-dependent behavior arises from whether H^+ or OH^- is preabsorbed onto the surface of noble metal nanozymes, which dictates the energy barriers of H_2O_2 decomposition pathways. As shown in Fig. 4B, when these noble metal nanozymes preabsorb H* (* denotes being absorbed to the nanozyme surface), H_2O_2* would prefer a base-like decomposition pathway to generate two OH*, which will become H_2O* and O* in the presence of H*. O* is extremely oxidizing and will attack H-donors in the vicinity, such as TMB molecules. Collectively, this process consumes one H_2O_2 and oxidize a substrate molecule by generating •OH radicals, emulating the catalytic behavior of a peroxidase. Alternatively, when noble metal nanozymes pre-absorb OH* under basic conditions, H_2O_2* undergoes an acid-like decomposition and generate H_2O* and HO_2*. The latter will react with another H_2O_2* and produce H_2O*, H_2O_2* and O_2. In total, two H_2O_2 molecules yield two H_2O and one O_2, a reaction that defines the catalase activity of noble metal nanoparticles. The reaction rates for H_2O_2 decomposition follow an decreasing order of Au(111) < Ag(111) < Pd(111) < Pt(111) in equivalent acidic and basic conditions. Moreover, the established findings were used to predict the enzyme activity and reaction products of several metal hybrids under different pH conditions. Experimental results agreed well with calculations, showing an increasing peroxidase-like activities of metal nanorods as follows: Au@Ag < Au < Au@Pd < Au@Pt. Later, Gao and co-workers found that the metal composition and exposed facets of metal ions dictated the oxidase and SOD-like activities of metal and alloy-based nanozymes (Fig. 4C and D).[23] The absorption and dissociation energy of O_2 to yield single-atomic oxygen is the rate-determining step for oxidase-mimicking of metal nanozymes. As for the SOD-like activity, the protonation energy of superoxide radicals on the metal nanozyme surface determines the dismutation rate.

In 2011, Bradley and co-workers prepared palladium nanoparticles embedded on polystyrene microspheres for intracellular biorthogonal reactions, including allylcarbamate cleavage and Suzuki-Miyaura cross-coupling.[24] The idea of Pd^0 nanozyme mediated hydrolysis of allylcarbamate evolved from an earlier study where researchers applied a water-soluble ruthenium complex for intracellular catalysis. Nanozymes are preferred to molecular catalysts as they elicit minimal toxicity, exhibit better biosafety and have a more sustained chemical performance. It's worth noting that no natural enzymes were capable of such reactions.

The size of Pd^0 nanozyme is around 500 nm, far exceeding the size of proteins and may thus interfering with normal cellular metabolism. On account of this, Rotello and co-workers fabricated transition metal (Ru and Pd) encapsulated gold nanozymes featuring a size of around 10 nm (Fig. 4E).[25] Ru/Pd containing small molecule catalysts were encapsulated in the AuNP monolayer and remain active. To allow activation and deactivation of this nanozyme, cucurbit[7]uril was added to block the active sites of Ru/Pd catalysts. Upon adding of 1-adamantylamine, the nanozyme can be fully restored and elicit maximum catalysis. Kinetic profiling of this nanozyme showed that the K_M was 0.83 ± 0.09 μM with a k_{cat} of 1.07×10^5 s^{-1} (Fig. 4F). Live cell imaging and intracellular prodrug activation could be achieved using this nanozyme with on/off control.

3.2 Cu$_2$O nanozyme

Cuprous oxide (Cu$_2$O) nanoparticles were found to mimic the enzyme behaviors of GOx, HRP, lactase and cytochrome c oxidase when supported with polypyrrole, carbon dots or even in its bare form. Similar hydrothermal methods were applied to reduce copper ions into cuprous oxide nanomaterials with the presence of polymer molecules in basic conditions. Co-heating Cu (NO$_3$)$_2$ with pyrrole and NaOH at 80 °C for 1 h may generate Cu$_2$O@polypyrrole.[26] In strongly basic solutions, this nanozyme first accepts electrons from oxygen, oxidize glucose molecules and produce hydrogen peroxide. Then, the HRP-like activity of Cu$_2$O@polypyrrole converts H$_2$O$_2$ into hydroxyl radicals *via* a Fenton-like reaction (Fig. 5A).

In addition to glucose oxidase and peroxidase mimicking, the Cu^{2+}/Cu^{1+} redox couple affords cuprous oxide nanoparticles laccase and cytochrome c oxidase properties. Natural laccase is an oxidase that catalyzes the oxidation and crosslinking of phenols. Distinct from oxidases that convert oxygen to water and H$_2$O$_2$, laccase catalyzes oxygen to water without the production of H$_2$O$_2$. Cu$_2$O supported by carbon nanodots could reduce oxygen to water and oxidize hydroquinone and p-phenylenediamine to produce colorimetric reactions for biosensing.[27] The catalytic role of Cu was highlighted by the lack of enzyme-like activity of carbon dots alone. Later, Liu and co-workers used copper-containing MOF to replicate the active centers of laccases (Fig. 5B).[28] Cu^{2+} ions were chelated with different nucleobases where guanosine monophosphates (GMP) was determined the best. This Cu/GMP nanozyme proves a rivalry of natural laccase and does not generate H$_2$O$_2$. Free Cu^{2+} in the solution did not elicit a similar catalytic reaction. When GMP chelated other metal ions including Tb^{3+}, Gd^{3+}, Zn^{2+} and Fe^{2+}, among others, nanozyme activity decreased dramatically, emphasizing the critical role of Cu^{2+} as the essential metal ion for catalysis.

3.3 Nanoceria

Nanoceria promises many applications in biomedical fields as anti-oxidant nanozymes due to its excellent properties as SOD, oxidase and catalase mimics (Fig. 5C and D).[29] McGinnis and co-workers applied nanoceria as SOD mimics to protect photoreceptor cells and prevent light-induced retinal degeneration in rats.[15] When forming nanoceria, oxygen vacancies emerge and Ce^{3+}/Ce^{4+} flip-flops may initiate catalytic reactions shown in Fig. 5C. Formation of H$_2$O$_2$ as a product and competition study using ferricytochrome C both confirmed the SOD-mimicking properties of nanoceria. Investigation on mechanisms showed that nanoceria with a higher ratio of Ce^{3+} demonstrated higher catalytic activity. The catalytic rate constant was determined to be 3.6×10^9 M^{-1} s^{-1}, slightly higher than that of natural CuZn-SOD (1.3–2.8×10^9 M^{-1} s^{-1}).

Perez and co-workers reported that polymer coated nanoceria presented oxidase activity under acidic pH.[30] Their results suggested that no SOD or catalase activity was found since H$_2$O$_2$ was not needed for the reaction. The polymer coated nanoceria showed universal oxidase activity toward TMB, ABTS and DOPA in a pH-dependent manner while optimal performance was found at pH 4.0. The oxidase-mimicking properties depended on the pH, the size of the nanoceria, and the thickness of the polymer coating. A smaller nanoceria core and thinner polymer coating improved oxidation. These increases in catalytic efficiency

were attributed to the increased surface area to volume ratio and thinner and permeable coating that facilitates substrate molecule exchange. The catalytic rate constant for nanoceria was found to be 7×10^7 M^{-1} s^{-1} at pH 4.0, one magnitude faster than oxidation when using HRP in the presence of H_2O_2.

3.4 Melanin nanoparticles (MeNPs)

In 2017, Lu, Shi and co-workers demonstrated the multiple enzyme-mimicking activities of melanin nanoparticles as antioxidants for treatment of ischemic reperfusion brain injury.[32] Melanin, a biological polymer present in most living organisms including humans, is known for its intrinsic photoacoustic response and strong chelating ability to metal ions. PEGylated melanin nanoparticle (PEG-MeNP) can scavenge reactive oxygen and nitrogen species (RONS), namely superoxide ($O_2^{\bullet-}$), hydroxyl ($\bullet OH$), nitric oxide ($\bullet NO$) and peroxynitrite ($ONOO^-$) radicals. EPR spectroscopy, X-ray photoelectron spectroscopy and the generation of oxygen all together confirmed the SOD-mimicking behavior of PEG-MeNP. The turnover value k_{cat} was measured to be 2.16×10^5 s^{-1} and sustained catalytic activity was confirmed at different pH values (5, 7, and 9). It was also found that PEG-MeNP can react with H_2O_2 without the presence of other antioxidants such as glutathione. This indicates the possible catalase-like activity of melanin nanoparticles. The reaction of melanin nanoparticles with $\bullet OH$, $\bullet NO$ and $ONOO^-$ was also investigated. Results suggested that PEG-MeNP may effectively neutralize these radicals *via* nitration and nitrosation of phenolic groups abundant in melanin structures. However, a more detailed understanding of the mechanism is still needed.

3.5 Prussian blue nanoparticles (PBNPs)

Zhang, Gu and co-workers reported the multiple enzyme-like activities of PBNP, including peroxidase, catalase and SOD (Fig. 5E).[31] Prussian blue, with an idealized chemical form of $[Fe_2(CN)_6]^-$, could form PBNPs with polyvinylpyrrolidone (PVP) as a stabilizer. PBNP can catalyze the oxidation of TMB and ABTS in the presence of H_2O_2 at a pH of ~4.0, and this peroxidase-like activity was found higher than Fe_3O_4 nanoparticles reported previously. The peroxidase-mimicking property decreases as the pH environment shifts from acidic to neutral. Alternatively, oxygen was produced and a catalase-like activity of PBNP was demonstrated. The production of oxygen was found proportional to the PBNP concentration. PBNP was also found to be SOD-mimicking at different pH values as EPR spectrum confirmed the existence of $\bullet OOH$ radicals during reactions. Mechanism studies suggest that pH environments dictate the redox potentials of Prussian Blue to Prussian Yellow, Prussian White, or Berlin Green ($Fe_2(CN)_6$, $[Fe_2(CN)_6]^{2-}$, and $Fe_3[Fe(CN)_6]_2[Fe(CN)_6]^-$, respectively) where the valences of Fe changes as the electrons transfer among H_2O_2, O_2 and super-oxide radicals.

4 Biomedical applications of nanozymes

Many nanozymes have already proven competitive rivals to the natural enzyme they mimic. The emerging discovery and deeper understanding of nanozyme systems have enabled more biomedical applications, ranging from *in vitro* biosensing of biomarkers to *in vivo* imaging and therapy of various diseases. Unsatisfied with using nanozymes as standalone surrogates

of natural enzymes, multifunctional nanozyme systems allowed for increasing responsive applications with more synergies. This section highlights various types of biomedical applications that nanozymes have been currently involved in. By categorizing nanozymes into three subtypes based on their mode of application, including self-acting, synergistic, and remotely-controlled nanozymes, we demonstrate how nanozymes enable advances in biomedicine.

4.1 Self-acting nanozymes

Nanozymes were first applied in biosensing and colorimetric assays as direct surrogates of nature enzymes. Nanozymes have often provided additional properties that natural enzymes could not offer. As one of the most used methods for biomarker detection, ELISA normally uses HRP, a peroxidase, to oxidize TMB for color development and subsequent quantification. However, as a protein-based enzyme, HRP is limited to a nartr range of pH, temperature and concentration due to its instability in harsh conditions and high cost. Nanozymes have emerged to provide excellent substitutes while offering better tolerance to pH environments and temperature, higher amount/concentration when needed, and even increased catalytic efficiencies in some cases. Moreover, the programmability of nanozymes may allow researchers to design and control the activation or deactivation of catalysis reactions.

Fe_3O_4 magnetic nanoparticles, nanoceria, graphene oxide nanosheets and many peroxidase-mimicking nanozymes can all challenge HRP in biosensing processes. Additionally, these materials have advantageous intrinsic properties that may further facilitate research. For example, most nanozymes can be centrifuged down to separate themselves from the solution for analysis or recycling, which is difficult for protein enzymes. Fe_3O_4 nanozyme possess both peroxidase-mimicking activity and magnetism, which render it ideal for ELISA analysis where no HRP is needed for color development and colorimetric analysis. We first developed this method to enrich cardiac troponin 1 in serum for myocardial infarction detection.[4] With only a magnet, target antigens can be easily separated and collected from biological samples. Later, in the presence of H_2O_2 and TMB, antigen-bearing Fe_3O_4 MNP readily catalyzed the color reaction for quantification.

Fe_3O_4 nanozyme coated with a recombinant human heavy-chain ferritin (HFn) protein shell can target most cancer cells overexpressing transferrin receptor 1 (Fig. 6A–D).[33] After applying HFn-Fe_3O_4 to tumor tissue slides, cancerous regions can be visualized using DAB and H_2O_2. Owing to the high catalytic performance of Fe_3O_4 and broad targeting spectrum of HFn, nine types of cancer cells were identified among 474 clinical human specimens with a specificity of over 95% and sensitivity of 98%.

Nanozymes allow biosensing applications tailored for their specific properties other than providing simple purification *via* magnetism and centrifugation. Researchers developed label-free single-nucleotide polymorphism (SNP) detection systems using carbon-based nanozyme, such as SWNT and GO, to mimic natural HRP.[34] Single-stranded DNA (ssDNA) has a high affinity to carbon nanozymes *via* π–π stacking and hydrogen bonds. Such binding may prevent carbon nanozymes from salt-induced precipitation while double-stranded DNA (dsDNA) proved ineffective. Taking advantages of this property and

programmable DNA hybridization, fully hybridizable DNA strands and mutated strands with a single base mismatch may be readily differentiated (Fig. 6E). A general procedure may start with absorbing a target ssDNA onto carbon nanozymes. Increasing salt concentration will generate different extents of aggregation when adding DNA strands of interest. Full hybridization produces the highest amount of precipitates. Either the supernatant or precipitate can be analyzed in the presence of TMB and hydrogen peroxide to develop a colorimetric reaction. A stronger blue color indicates a higher concentration of carbon nanozyme and less DNA mutation when analyzing the precipitate (Fig. 6F). The lowest detection limit was found to be approximately 1 nM. This label-free SNP detection system using carbon nanozymes showed advantages over natural HRP since carbon nanomaterials are intrinsically catalytic and they have special interactions with DNA strands.

Since most nanozymes work as oxidoreductases, they are involved in many redox reactions and can be used for ROS scavenging purposes. V_2O_5 nanozyme behaves intrinsic vanadium haloperoxidase (V-HPO) and glutathione peroxidase (GPx) activity. Mugesh and co-workers first tested its selectivity at the presence of both substrates (iodine as the V-HPO substrate and GSH as the GPx substrate).[12] Results indicated that the GPx activity of V_2O_5 nanozyme was not affected due to the high affinity of GSH to polarized oxygen atoms on the surface of V_2O_5 nanozyme. V_2O_5 nanozyme enters cells through endocytosis and scavenges intracellular ROS through its enzyme-mimicking ability *via* the cooperation with glutathione reductase to complete the recycle of glutathione and glutathione disulfide.

MoO_3 nanozyme was found to be useful for cell detoxification by acting as a sulfite oxidase mimic. Lack of natural or artificial sulfite oxidase was associated with neurological damage and early childhood death.[18] After modifying with triphenylphosphonium ions, MoO3 nanozyme with a size of around 2 nm can actively target mitochondria and alleviate oxidative stress due to sulfite oxidase deficiency (Fig. 7A). Tour and co-workers applied PEG functionalized hydrophilic carbon clusters as antioxidants for traumatic brain injury protection (Fig. 7B).[35] PEGylated melanin nanoparticle (PEG-MnNP) with multiple enzyme-mimicking activities found its application for ischemic brain injury prevention.[32] After intracranial injection into the brain, PEG-MnNP can scavenge various types and a large amount of reactive oxygen and nitrogen species in the vicinity of brain injury sites. The local administration of PEG-MnNP into lateral ventricles effectively decreased infarct area from ~32% in the untreated group to ~14% (Fig. 7C).

Other than neutralizing ROS, some nanozymes may aid in the process of producing active radicals for treatment purposes. Pd nanozymes exhibited oxidase and peroxidase-like activities and were used against Gram-positive and Gram-negative bacteria *via* generation of ROS.[36] Zhou and co-workers found that Pd(111) octahedrons showed stronger anti Gram-negative bacteria activities than Pd(100) cubes. The Pd(100) nanozyme presented higher anti Gram-positive performance than Pd(111). Mechanism studies demonstrated that Pd(100) nanozyme has a higher affinity toward O_2 or H_2O_2 molecules, making it a stronger oxidase and peroxidase-mimicking nanozyme. However, Pd(111) showed increased penetration inside bacteria to fully elicit its anti-bacterial activity.

Koo and co-workers used ferumoxytol in combination with low concentration of H_2O_2 to combat oral biofilms and prevent dental decay.[37] Ferumoxytol, carboxymethyl dextran-coated iron oxide nanoparticles, can act as intrinsic peroxidase-like nanozyme and catalyze the decomposition of H_2O_2 to hydroxyl radicals. The reaction presented the highest activity at pH 4.5 but are dormant at pH 6.5 (Fig. 8A–C). This pH-responsive property of ferumoxytol nanozyme makes it ideal for targeting acidic biofilms but also friendly to healthy teeth (Fig. 8D–F).

4.2   Synergistic nanozymes

Although nanozymes were discovered for their independent enzyme-like activity, efforts in recent years have been geared towards highly-ordered synergistic application of nanozymes in cascade systems for biomedical purposes. By revisiting how the fundamental characteristics of an environment, such as pH, glutathione and hydrogen peroxide concentrations as well as levels of oxygenation, may shed influences on nanozyme performances. In turn, we can better adjust the subsequent diagnostic and therapeutic role of nanozymes. In this section, we illustrate the design of nanozymes in coordination with other nanozymes, natural enzymes, or nanomaterials for synergetic purposes, from biosensing to theranostics, from *in vitro* to *in vivo*.

For in *vitro* biosensing, Xu *et al.* modified carbon fiber microelectrodes with two nanozymes: graphene quantum dots (GQDs) and AuPd alloy nanoparticles.[38] The excellent electrocatalytic activity of GQDs for H_2O_2 decomposition stems from their aromatic structure and abundant carboxylic groups on the surface. In addition, the quantum confinement and edge effects of GQDs greatly facilitated the nucleation and formation of high-density AuPd nanoparticles on carbon fiber microelectrodes, further improving the overall peroxidase activity of the sensor. The as-prepared microelectrode showed a wide liner detection range from 1.0 μM to 18.4 mM, with a low limit of ~0.5 μM (signal-to-noise ratio S/N = 3). This sensor also showed differentiated response to varying levels of H_2O_2 in live human breast cancer cells and presented excellent sensitivity and selectivity in *in situ* tracking of H_2O_2 at trace amount in clinical breast cancer tissues.

Based on the intrinsic peroxidase-mimicking properties of graphene oxide (GO), Qu and co-workers established a novel means for glucose concentration measurement.[10] Given the fact that hydrogen peroxide could be produced by glucose oxidase (GOx) in the presence of glucose, the colorimetric measurement of glucose concentration could be achieved by synergistic cooperation of GOx and GO. The reaction was traditionally realized by using HRP. However, GOx–GO nanozyme systems provided excellent selectivity toward glucose and GO offered higher affinity to TMB molecules than normal HRP and ferrimagnetic nanoparticles *via* π–π stacking and hydrophobic interactions.

Zhang and co-workers further developed this cascade catalysis using AuNP loaded Cu-TCPP(Fe) MOF nanosheets, since the former is GOx-mimicking and the latter can act as a natural peroxidase (Fig. 9A).[39] MOF serves as the template for AuNPs to grow on and accepts H_2O_2 from AuNP oxidization of glucose (Fig. 9B). A good linear relationship to the glucose concentration has been shown and the detection limit can reach down to 8.5 –M.

The change from natural GOx to AuNP nanozyme made the cascade reaction more tolerant to different pH conditions and offers more options for glucose detection.

Xia and co-workers developed a three-in-one nanozyme system for controlled self-assembly, fluorescent sensing, and cascade catalysis using cyclodextrin (CD) functionalized AuNP, or CD@AuNP (Fig. 9C and D).[40] The addition of TCPP molecules initiates self-assembly of CD@AuNP into 1D or 2D superstructures. Cyclodextrin molecules on the surface of gold nanoparticles may trap rhodamine B and quench its fluorescence. In the presence of cholesterols, the trapped rhodamine B dye is released and the fluorescent signal recovers. This property enabled the sensitive and specific detection of cholesterols (such as β-sitosterol) in blood samples, with a detection limit of 1.5 μM and a S/N ratio of ~3. Given the GOx and HRP-mimicking enzyme activities of AuNP, CD@AuNP nanozyme was also found to oxidize glucose into gluconic acid and produce H_2O_2 at pH 9. Alternatively, CD@AuNP may catalyze the oxidation of TMB using H_2O_2 at pH 4.5. Collectively, a cascade catalysis could be designed using CD@AuNP to first oxidize glucose and generate H_2O_2, which was then carried over to oxidize TMB to produce a colorimetric reaction. A pH-regulated, self-synergistic AuNP nanozyme like this unveiled many useful properties of nanozymes for biosensing. Moreover, CD@AuNP nanozyme also suggested design strategies to manipulate the behavior of nanozymes by controlling their surface moieties.

In 2017, Shi, Chen and co-workers further developed a combination therapy using GOx and magnetic iron oxide nanoparticles for *in vivo* cancer treatment.[41] They conceived a sequential nanozyme system where biodegradable silica nanoparticles carried GOx and ultrasmall Fe_3O_4 nanoparticles. Tumor microenvironments feature a high concentration of glucose and mildly acidic environment. When this nanozyme reaches tumor sites *via* EPR effects, GOx will first consume glucose to produce H_2O_2, which will be then catalyzed by peroxidase-like Fe_3O_4 nanoparticles to generate highly toxic hydroxyl radicals near tumor cells (Fig. 9E–G). This work highlights how nanozymes can be used synergistically for cancer theranostics and emphasizes the importance of deeper understanding of the central characteristics of tissue microenvironment. Physiological changes of diseases, and more importantly, hallmarks of cancer, may shed significant insights on subsequent diagnostic and therapies.

Traditional photodynamic therapy (PDT) applies light-generated ROS to suppress tumor growth. However, as the source of ROS, O_2 is not abundant in the vicinity of tumors due to hypoxia. In fact, the implementation of PDT might increase the degree of hypoxia and limit the efficacy of PDT as well as chemo- and radiotherapy. Manganese ferrite nanoparticles (MFNs) can work as a catalase to accelerate the dismutation of H_2O_2 *via* a Fenton-like mechanism (Fig. 10).[42] After its delivery to tumor sites, the MFN-loaded mesoporous silica nanoparticles can constantly produce O_2 to alleviate hypoxia and make PDT treatment more efficacious. Additionally, MFN can also serve as an MRI contrast agent, allowing non-invasive tracking of the nanozyme *in vivo.* Thus, MFNs proved a promising theranostic nanozyme for cancer therapy.

Gao, Yan and co-workers developed a N-doped porous carbon nanozyme for cancer treatment *via* ROS regulation (Fig. 11).[43] This nanozyme could mimic four different natural

enzymes, including oxidase, catalase, SOD and peroxidase. In the tumor microenvironment, N-doped carbon nanozyme may increase intracellular ROS levels, consume oxygen and produce hypoxia, which all lead to tumor cell death. After modifying with human H-ferritin, N-doped carbon nanozyme successfully reached tumor sites and was delivered into lysosomes *via* receptor-mediated endocytosis. The acidic environment initiated the oxidase and peroxidase-like activities and generated ROS. Intravenous injection of this nanozyme showed excellent anti-tumor effects in mice bearing HepG2 tumors.

4.3 Nanozymes with remote control

To facilitate more accurate control, highly responsive catalytic nanozyme systems have been developed to be activated by external stimuli, such as light, heat, ultrasound, or magnetic fields. Herein, we list these nanozymes and their applications with an emphasis on strategies for the future development of nanozymes for biomedical applications with excellent temporal and spatial precision.

Light is one of the earliest and most commonly used methods to trigger or regulate a catalytic reaction. It can be delivered with high accuracy and controllability. By tuning the wavelength, different nanozyme effects are triggered. Prins and co-workers designed a light-regulating AuNP nanozyme for RNA hydrolysis.[44] When modified with Zn^{2+} chelated triazacyclononane molecules, AuNP nanozyme may boost the hydrolysis of the model RNA molecule, 2-hydroxypropyl *p*-nitro-phenyl phosphate (HPNPP). The catalysis can be controlled by Zn^{2+} chelation ratios, addition of inhibitors, and AuNP binding molecules. 4-(Phenylazo) benzoic acid is a photo-sensitive co-factor that will shift between *cis* and *trans*-forms upon 365 and 465 nm light irradiation (Fig. 12A and B). In its *trans*-form, this co-factor has a higher affinity to AuNP nanozyme and may inhibit the binding of HPNPP substrates and therefore the hydrolysis reaction. The addition of a light-sensitive co-factor into a nanozyme system composed an elegant example of how light may be used to regulate nanozyme performance.

A similar design was adopted by Qu and co-workers. They surface-engineered transition metal nanozymes to be light-responsive (Fig. 12C).[45] Such a nanozyme can catalyze the hydrolysis of allylcarbamates in a biorthogonal fashion, which could be used for live cell imaging. Transition metal nanospheres were imbedded inside silica nanoparticles and further modified with azobenzene as the light switch. The as-formed nanozyme systems can be silenced by cyclodextrin *via* active site blocking. UV light irradiation may recover the nanozyme by removing the cyclodextrin. Under visible light, the cyclodextrin blocking would be active again. This light-triggered nanozyme systems proved effective for multiple transition metals related to the hydrolysis process, including Ru, Pd and Rh. Additionally, this activation/deactivation cycle can be repeatedly used, allowing maximum control over the intracellular catalysis. Moreover, minimal dose of UV light was needed for the transformation of azobenzene to turn on the reaction. The responsive transition metal nanozyme systems demonstrated its great potential on designability and the light-triggered design allowed maximum controllability.

Inflammation is commonly associated with ROS, with hydroxyl radicals proposing the highest threat. Inspired by natural photosynthesis and the fact that hydrogen gas can reduce

•OH into water, Chia, Sung and co-workers assembled a multicomponent system to produce H_2 gas in close proximity to the inflammation site in mice (Fig. 13A).[46] Chlorophyll a, ascorbic acid and gold nanoparticles were sealed inside liposomes and used as the photosensitizer, electron donor, and hydrogenase-mimicking nanozyme, respectively. This nanozyme system may produce hydrogen only upon light irradiation at 660 nm and mitigate cellular damage caused by ROS *in vitro.* After local injection into the inflamed sites in mice, this nanozyme system fought against ROS effectively.

Fullerenes have long been established as a SOD-mimicking nanozyme with the ability to absorb ROS *in vitro* and *in vivo.* Qu and co-workers later found that UV or visible light may excite fullerenes to produce ROS and yield superoxide radicals and singlet oxygen through pathways of electron transferring.[47] Fullerene were thus applied to light-controlled therapy of Alzheimer's disease (AD) after modifying with active targeting peptides and UCNP. Upon light irradiation, UCNP can transfer energy from NIR light to excite fullerenes to produce ROS. The presence of ROS will slow down amyloid-β peptide (Aβ) aggregation and mitigate AD progression. To avoid side effects of excessive ROS *in vivo*, fullerenes in the dark will scavenge ROS effectively to minimize the photo-toxicity of fullerene and potential detrimental effects (Fig. 13B). This fullerene nanozyme was tested in AD models of *Caenorhabditis elegans* (*C. elegans*) and showed excellent neuroprotection against Aβ aggregation. Moreover, UCNP in this nanozyme systems served as an MRI contrast agent and provided image guidance for the treatment.

Heat presents another stimulant to trigger nanozymes. Nie, Xia and co-workers developed a heat-triggered, enzyme-free signal amplification technique. They utilized gold vesicles encapsulated with Pd–Ir nanoparticles as peroxidase mimics for colorimetric assay of disease biomarkers (Fig. 13C).[48] Pd–Ir nanoparticles were sheltered by gold vesicles, which may break down upon heating and release the encapsulated Pd-Ir nanozyme. This nanozyme system showed significantly improved catalytic efficiency. The detection limit reached down to the femtogram per mol level, 1000-fold lower than that of the conventional enzyme-based technique. Traditional methods to improve colorimetric assay efficiency generally relied on attaching natural enzymes onto individual carriers which is ultimately limited to the number of binding and the catalytic efficiency of enzymes. These inherent problems could be solved by applying nanozyme systems to speed the catalytic process.

Qu and co-workers engineered a heat-regenerating logic gate using nanoceria as the signal transducer (Fig. 13D).[49] As a SOD-mimicking nanozyme, colorless nanoceria may turn yellow in the presence of H_2O_2 due to the Ce^{3+} to Ce^{4+} transition on the surface of the nanozyme. The color of nanoceria can thus be used as an output when other cooperating enzymes are added. When GOx and β-galactosidase are used as input enzymes, lactose in the solution may generate H_2O_2 and oxidize nanoceria to turn yellow. This cascade may only function when all the components are present, and the output is set as "AND". Any missing component would cause no color change of nanoceria and set the logic gate to an "OFF" state. When adding either GOx or xanthine oxidase as inputs, the color change of nanoceria may constitute an "OR" gate, since only one of the enzymes is needed to produce H_2O_2. Additionally, adding catalase may generate the "INHIBIT" gate with no color change

as the output signal. Most intriguingly, this logic gate system can be reset thermally since all the inputs are heat-sensitive natural enzymes while nanoceria is inert to heat.

Other than light and heat, ultrasound can also be used as a stimulus for nanozymes. Yeh and co-workers reported an H_2O_2-encapsulated Fe_3O_4-PLGA polymer nanozyme system for cancer therapy.[50] After accumulating into tumor sites *via* passive targeting and magnetism-mediated active targeting, the polymer system can be disrupted by external energy from the diagnostic ultrasound. Upon ultrasound activation, H_2O_2 will be released and reacts with Fe_3O_4 nanoparticles for oxygen and hydroxyl radical production. The oxygen can enhance the imaging sensitivity of ultrasound, while overproduced hydroxyl radicals can enhance local oxidative stress for tumor suppression. Additionally, this Fe_3O_4-containing nanocomplex also served as the MR contrast agent, offering non-invasive guidance of sonodynamic therapy and treatment monitoring afterward.

5 Conclusion and perspectives

Nanozymes have gathered increasing amounts of research interest due to their superior catalytic properties and improved tolerance to harsh conditions that natural enzymes cannot endure. Nanozymes rapidly impressed researchers as direct substitutes of natural enzymes in biosensing fields. Moreover, the intrinsic physiochemical properties of nanosystems endow nanozymes more possibilities to work synergistically with the environment and thus be responsive to various biomedical settings. Different pH values, redox conditions, and levels of oxygenation (such as hypoxia in tumors) can significantly alter the catalytic behavior of nanozymes. Additionally, exogenous energy sources in forms of light, heat, ultrasound or magnetic fields may influence nanozymes with rational design. The versatility of nanozymes has catalyzed innovation and creativity in the fields of biomedicine.

As our understanding of diseases and nanotechnology deepens, potential biomedical applications of nanozymes broaden. The future of nanozymes in biomedical applications holds excellent promise especially in the area of disease early detection, deep tissue imaging, responsive drug delivery as well as multifunctional precision therapy. Even though notable progress has been made in the bioengineering of nanozymes, this field is still in its infancy and faces many challenges.

(1) The catalytic profiles of different nanozymes should be fully investigated. Specific mechanisms will have to be comprehensively understood to allow more control over the reactions. For example, many nanozymes accept a broad range of substrates and therefore present multiple enzyme-mimicking activities. As delightful such a property might be, it will also give rise to concerns of catalytic specificity and substrate selectivity. Moreover, this might challenge our ability to govern multiple nanozymes synergistically.

(2) Rational design and surface chemistry of nanozymes are fundamental to determine their catalytic performance and, therefore, their biomedical applications. Many studies reported conflicting mechanisms of nanozymes for catalysis, such as nanoceria. This highlights the challenges of establishing standard catalytic profiles of nanozymes. Experimental and

computational studies can actively aid in the process of nanozyme design and mechanism investigations.

(3) Although nanozymes can be recycled and usually are not costly to produce, future applications are also expected for immobilization of nanozymes so they can be purified and regenerated.

(4) The types of nanozymes, which are generally limited to oxidoreductases and hydrolases, are still falling short to the full list of natural enzymes. Future developments of nanozymes are expected to expand their utilization into the numerous and diverse enzyme categories that exist.

(5) When administrated into living organisms, the biological fates of nanozyme systems should be systematically investigated. Unlike natural enzymes, the biocompatibility and biodegradability are common concerns of nanomaterials-based biomedicines.

(6) The search for stimulators and inhibitors of nanozymes in a biological context would be an exciting topic, which could be used to tailor the activity and behaviors of nanozymes.

(7) The replacement of protein enzymes in industrial and medical applications with nanozymes is getting closer; there is still more work to be done. How to improve the batch-to-batch reproducibility of nanozymes is vital for their industrial or clinical translation.

Acknowledgements

Biographies

Dawei Jiang received his PhD in inorganic chemistry from Shanghai Institute of Applied Physics (SINAP), Chinese Academy of Sciences in 2015. He then joined the University of Wisconsin – Madison for his postdoctoral training under the supervision of Prof. Weibo Cai. Dr Jiang has been dedicated to the rational design and biomedical applications of biomolecule-based radiopharmaceuticals, including proteins and DNA oligonucleotides, for imaging and therapy of cancer and kidney diseases.

Dalong Ni received his PhD degree in 2016 from the Shanghai Institute of Ceramics, Chinese Academy of Sciences (SICCAS). He then joined the Department of Radiology at the University of Wisconsin – Madison as a postdoctoral fellow under the supervision of Prof. Weibo Cai. His research interests focus on design, synthesis, and biomedical applications of multifunctional nanoplatforms for imaging and therapy applications.

Zachary T. Rosenkrans is currently a PhD student in the Pharmaceutical Sciences program at the University of Wisconsin – Madison, under the supervision of Prof. Weibo Cai. He previously received a BS in chemical engineering from the University of Kansas in Lawrence, KS. His research is focused on developing nanomaterial-based platforms for image-guided drug delivery and theranostics.

Peng Huang received his PhD in Biomedical Engineering from the Shanghai Jiao Tong University in 2012. He then joined the Laboratory of Molecular Imaging and Nanomedicine (LOMIN) at the National Institutes of Health (NIH) as a postdoctoral fellow. In 2015, he moved to Shenzhen University (SZU) as a Distinguished Professor, Chief of the Laboratory of Evolutionary Theranostics (LET), and Director of the Department of Molecular Imaging. His research focuses on the design, synthesis, and biomedical applications of molecular imaging contrast agents, stimuli-responsive programmed targeting drug delivery systems, and activatable theranostics.

Xiyun Yan obtained her BS degree in 1983 from the Henan Medical College, and then studied cell biology in Professor Shizhang Bei's lab in the Institute of Biophysics, Chinese Academy of Sciences (CAS) until leaving for Germany in 1989. After receiving her medical

doctor's degree from Heidelberg University in Germany, she joined the Memorial Sloan-Kettering Institute in New York as a postdoctoral research fellow. In 1997, Dr Yan returned to China through her selection in the "Hundred Talents Program" by CAS. She has since studied tumor biology, finding novel targets and developing new methods for tumor diagnosis and therapy. Her work has been well recognized and respected internationally through honors such as the National Prize for Natural Science and Atlas Award by Elsevier.

Weibo Cai is a Vilas Distinguished Achievement Professor of Radiology/Medical Physics/Biomedical Engineering/Materials Science & Engineering/Pharmaceutical Sciences at the University of Wisconsin – Madison, USA. He received a PhD degree in Chemistry from UCSD in 2004. His research at UW – Madison is focused on molecular imaging and nanotechnology.

References

1. Wei H and Wang E, Chem. Soc. Rev, 2013, 42, 6060–6093. [PubMed: 23740388]

2. Wu J, Wang X, Wang Q, Lou Z, Li S, Zhu Y, Qin L and Wei H, Chem. Soc. Rev, 2019, 48, 1004–1076. [PubMed: 30534770]

3. Manea F, Houillon FB, Pasquato L and Scrimin P, Angew. Chem., Int. Ed, 2004, 43, 6165–6169.

4. Gao L, Zhuang J, Nie L, Zhang J, Zhang Y, Gu N, Wang T, Feng J, Yang D, Perrett S and Yan X, Nat. Nanotechnol, 2007, 2, 577–583. [PubMed: 18654371]

5. Nath I, Chakraborty J and Verpoort F, Chem. Soc. Rev, 2016, 45, 4127–4170. [PubMed: 27251115]

6. Sun H, Zhou Y, Ren J and Qu X, Angew. Chem., Int. Ed, 2018, 57, 9224–9237.

7. Chen Z, Wang Z, Ren J and Qu X, Acc. Chem. Res, 2018, 51, 789–799. [PubMed: 29489323]

8. Diez-Castellnou M, Mancin F and Scrimin P, J. Am. Chem. Soc, 2014, 136, 1158–1161. [PubMed: 24405094]

9. Mondloch JE, Katz MJ, Isley WC 3rd, Ghosh P, Liao P, Bury W, Wagner GW, Hall MG, DeCoste JB, Peterson GW, Snurr RQ, Cramer CJ, Hupp JT and Farha OK, Nat. Mater, 2015, 14, 512–516. [PubMed: 25774952]

10. Song Y, Qu K, Zhao C, Ren J and Qu X, Adv. Mater, 2010, 22, 2206–2210. [PubMed: 20564257]

11. Natalio F, Andre R, Hartog AF, Stoll B, Jochum KP, Wever R and Tremel W, Nat. Nanotechnol, 2012, 7, 530–535. [PubMed: 22751222]

12. Vernekar AA, Sinha D, Srivastava S, Paramasivam PU, D'Silva P and Mugesh G, Nat. Commun, 2014, 5, 5301. [PubMed: 25412933]

13. Cheng H, Liu Y, Hu Y, Ding Y, Lin S, Cao W, Wang Q, Wu J, Muhammad F, Zhao X, Zhao D, Li Z, Xing H and Wei H, Anal. Chem, 2017, 89, 11552–11559. [PubMed: 28992698]

14. Qin L, Wang X, Liu Y and Wei H, Anal. Chem, 2018, 90, 9983–9989. [PubMed: 30044077]

15. Chen J, Patil S, Seal S and McGinnis JF, Nat. Nanotechnol, 2006, 1, 142–150. [PubMed: 18654167]

16. Ali SS, Hardt JI, Quick KL, Kim-Han JS, Erlanger BF, Huang TT, Epstein CJ and Dugan LL, Free Radical Biol. Med, 2004, 37, 1191–1202. [PubMed: 15451059]

17. Samuel EL, Marcano DC, Berka V, Bitner BR, Wu G, Potter A, Fabian RH, Pautler RG, Kent TA, Tsai AL and Tour JM, Proc. Natl. Acad. Sci. U. S. A, 2015, 112, 2343–2348. [PubMed: 25675492]

18. Ragg R, Natalio F, Tahir MN, Janssen H, Kashyap A, Strand D, Strand S and Tremel W, ACS Nano, 2014, 8, 5182–5189. [PubMed: 24702461]

19. Grundner S, Markovits MA, Li G, Tromp M, Pidko EA, Hensen EJ, Jentys A, Sanchez-Sanchez M and Lercher JA, Nat. Commun, 2015, 6, 7546. [PubMed: 26109507]

20. Comotti M, Della Pina C, Matarrese R and Rossi M, Angew. Chem., Int. Ed, 2004, 43, 5812–5815.

21. Snyder BE, Vanelderen P, Bols ML, Hallaert SD, Bottger LH, Ungur L, Pierloot K, Schoonheydt RA, Sels BF and Solomon EI, Nature, 2016, 536, 317–321. [PubMed: 27535535]

22. Li J, Liu W, Wu X and Gao X, Biomaterials, 2015, 48, 37–44. [PubMed: 25701030]

23. Shen X, Liu W, Gao X, Lu Z, Wu X and Gao X, J. Am. Chem. Soc, 2015, 137, 15882–15891. [PubMed: 26642084]

24. Yusop RM, Unciti-Broceta A, Johansson EM, Sanchez-Martin RM and Bradley M, Nat. Chem, 2011, 3, 239–243. [PubMed: 21336331]

25. Tonga GY, Jeong Y, Duncan B, Mizuhara T, Mout R, Das R, Kim ST, Yeh YC, Yan B, Hou S and Rotello VM, Nat. Chem, 2015, 7, 597–603. [PubMed: 26100809]

26. Periasamy AP, Roy P, Wu WP, Huang YH and Chang HT, Electrochim. Acta, 2016, 215, 253–260.

27. Ren X, Liu J, Ren J, Tang F and Meng X, Nanoscale, 2015, 7, 19641–19646. [PubMed: 26548709]

28. Liang H, Lin F, Zhang Z, Liu B, Jiang S, Yuan Q and Liu J, ACS Appl. Mater. Interfaces, 2017, 9, 1352–1360. [PubMed: 28004568]

29. Celardo I, Pedersen JZ, Traversa E and Ghibelli L, Nanoscale, 2011, 3, 1411–1420. [PubMed: 21369578]

30. Asati A, Santra S, Kaittanis C, Nath S and Perez JM, Angew. Chem., Int. Ed, 2009, 48, 2308–2312.

31. Zhang W, Hu S, Yin JJ, He W, Lu W, Ma M, Gu N and Zhang Y, J. Am. Chem. Soc, 2016, 138, 5860–5865. [PubMed: 26918394]

32. Liu Y, Ai K, Ji X, Askhatova D, Du R, Lu L and Shi J, J. Am. Chem. Soc, 2017, 139, 856–862. [PubMed: 27997170]

33. Fan K, Cao C, Pan Y, Lu D, Yang D, Feng J, Song L, Liang M and Yan X, Nat. Nanotechnol, 2012, 7, 459–464. [PubMed: 22706697]

34. Song Y, Wang X, Zhao C, Qu K, Ren J and Qu X, Chem. – Eur. J, 2010, 16, 3617–3621. [PubMed: 20191629]

35. Bitner BR, Marcano DC, Berlin JM, Fabian RH, Cherian L, Culver JC, Dickinson ME, Robertson CS, Pautler RG, Kent TA and Tour JM, ACS Nano, 2012, 6, 8007–8014. [PubMed: 22866916]

36. Fang G, Li W, Shen X, Perez-Aguilar JM, Chong Y, Gao X, Chai Z, Chen C, Ge C and Zhou R, Nat. Commun, 2018, 9, 129. [PubMed: 29317632]

37. Liu Y, Naha PC, Hwang G, Kim D, Huang Y, Simon-Soro A, Jung HI, Ren Z, Li Y, Gubara S, Alawi F, Zero D, Hara AT, Cormode DP and Koo H, Nat. Commun, 2018, 9, 2920. [PubMed: 30065293]

38. Xu Q, Yuan H, Dong X, Zhang Y, Asif M, Dong Z, He W, Ren J, Sun Y and Xiao F, Biosens. Bioelectron, 2018, 107, 153–162. [PubMed: 29455025]

39. Huang Y, Zhao M, Han S, Lai Z, Yang J, Tan C, Ma Q, Lu Q, Chen J, Zhang X, Zhang Z, Li B, Chen B, Zong Y and Zhang H, Adv. Mater, 2017, 29, 1700102.

40. Zhao Y, Huang Y, Zhu H, Zhu Q and Xia Y, J. Am. Chem. Soc, 2016, 138, 16645–16654. [PubMed: 27983807]

41. Huo MF, Wang LY, Chen Y and Shi JL, Nat. Commun, 2017, 8, 357. [PubMed: 28842577]

42. Kim J, Cho HR, Jeon H, Kim D, Song C, Lee N, Choi SH and Hyeon T, J. Am. Chem. Soc, 2017, 139, 10992–10995. [PubMed: 28737393]

43. Fan K, Xi J, Fan L, Wang P, Zhu C, Tang Y, Xu X, Liang M, Jiang B, Yan X and Gao L, Nat. Commun, 2018, 9, 1440. [PubMed: 29650959]

44. Neri S, Garcia Martin S, Pezzato C and Prins LJ, J. Am. Chem. Soc, 2017, 139, 1794–1797. [PubMed: 28121141]

45. Wang F, Zhang Y, Du Z, Ren J and Qu X, Nat. Commun, 2018, 9, 1209. [PubMed: 29572444]

46. Wan WL, Lin YJ, Chen HL, Huang CC, Shih PC, Bow YR, Chia WT and Sung HW, J. Am. Chem. Soc, 2017, 139, 12923–12926. [PubMed: 28870078]

47. Du Z, Gao N, Wang X, Ren J and Qu X, Small, 2018, e1801852, DOI: 10.1002/smll.201801852. [PubMed: 30028575]

48. Ye H, Yang K, Tao J, Liu Y, Zhang Q, Habibi S, Nie Z and Xia X, ACS Nano, 2017, 11, 2052–2059. [PubMed: 28135070]

49. Lin Y, Xu C, Ren J and Qu X, Angew. Chem., Int. Ed, 2012, 51, 12579–12583.

50. Li WP, Su CH, Chang YC, Lin YJ and Yeh CS, ACS Nano, 2016, 10, 2017–2027. [PubMed: 26720714]

Key learning points

1. The innovative ideas of developing nanozymes from discovery to design

2. The new perspectives of exploring nanocomposites with intrinsic enzyme activity

3. The design strategies of nanozyme systems in response to one or multiple substrates

4. The representative biomedical applications of nanozymes in disease diagnosis and treatment

5. Outlook and potential challenges of future research and development
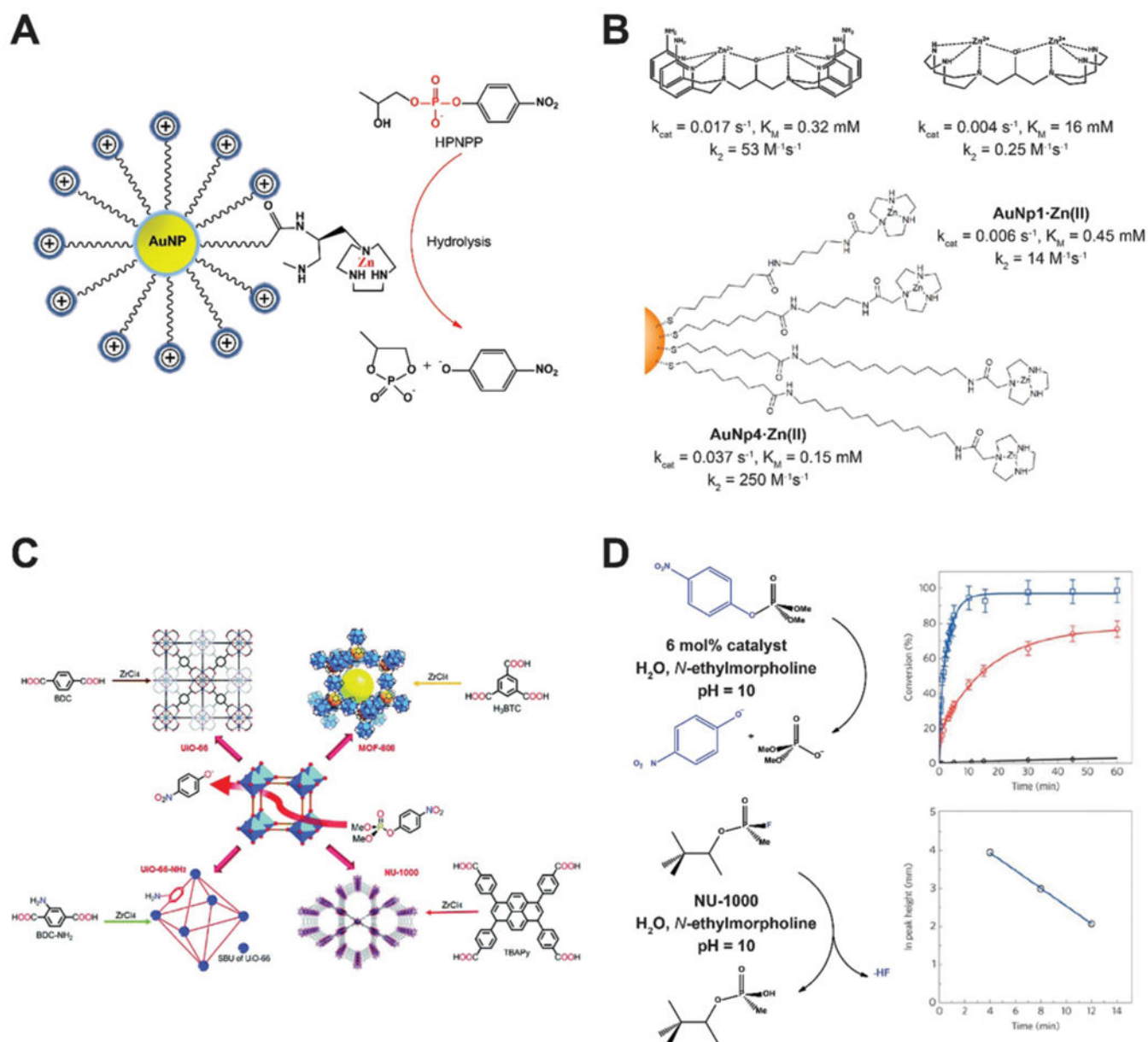
Fig. 1.
(A) AuNPs modified with triazacyclononane units can home Zn ions as metal ion centers to mimic phosphodiesterase (PDE). (B) Kinetic profiles of AuNP nanozymes with different side chain modifications in comparison with benchmark HPNPP cleaving bimetallic molecules. Reproduced from ref. 8 with permission from American Chemical Society, copyright 2014. (C) Phosphotriesterase (PTE) like MOF nanozymes hydrolyze a nerve agent simulant dimethyl 4-nitrophenyl phosphate (DMNP). The Zr–OH–Zr moieties established in MOFs mimic the active sites of PTE. Reprinted from ref. 5 with permission from the Royal Society of Chemistry, copyright 2016. (D) Reaction conditions for the hydrolysis of DMNP (upper row) and GD (lower row) in the presence of NU-1000 MOF nanozyme. Time-dependent conversion of DMNP using hydrated (red line) and dehydrated (blue line)

NU-1000 were shown in comparison with the background hydrolysis rate (black line). Hydrolysis of GD as a function of time is shown at the lower right panel. Reprinted from ref. 9 with permission from American Chemical Society, copyright 2015.
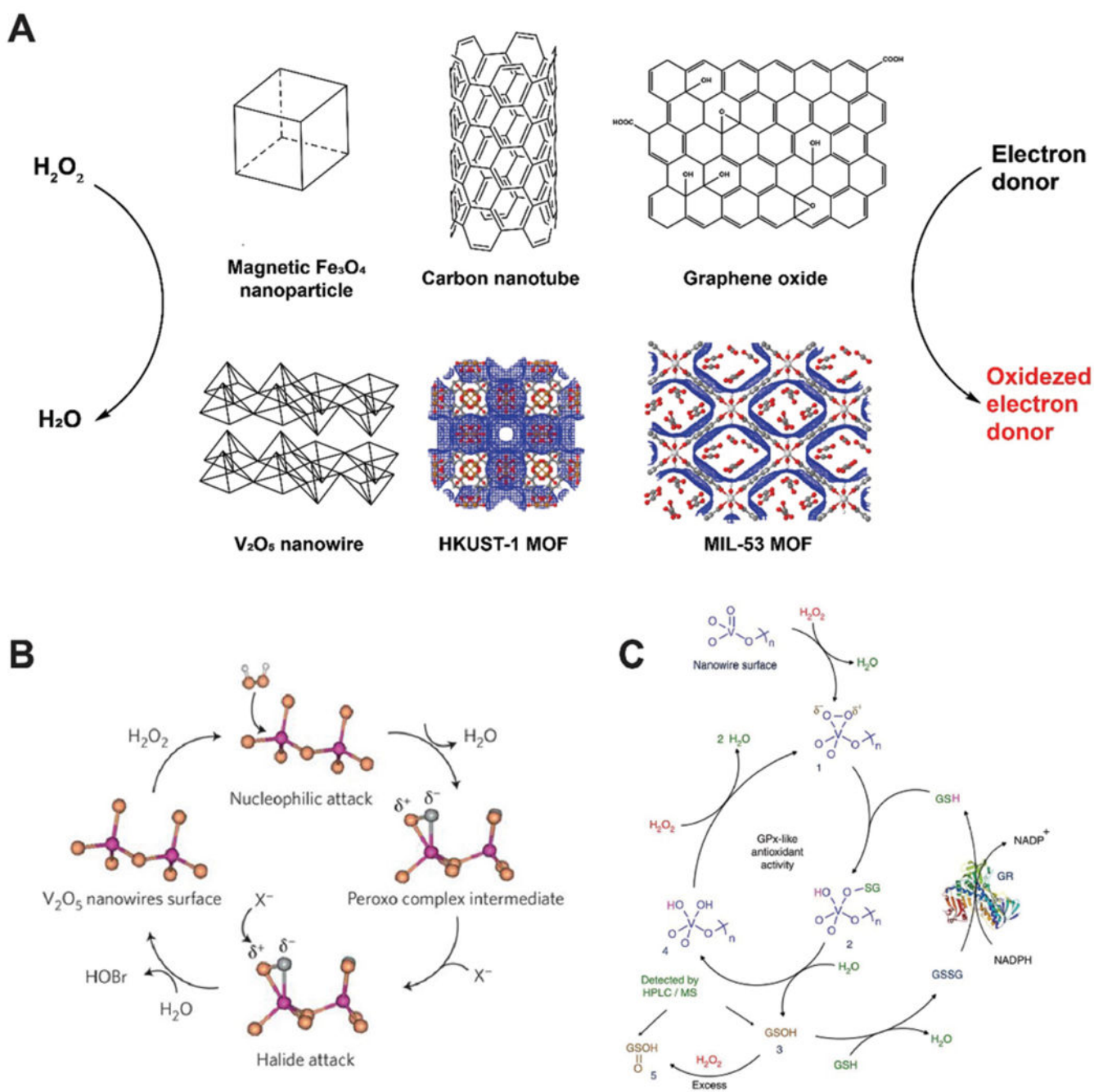
Fig. 2.
(A) Schematic of several peroxidase-mimicking nanozyme systems that catalyze the oxidation of electron donors in the presence of hydrogen peroxide. MOF structures were generated on www.ChemTube3D.com (B) V_2O_5 nanowire presents vanadium haloperoxidase-like activity and accelerates the transformation of bromide into HOBr. Reprinted from ref. 11 with permission from Springer Nature, copyright 2012. (C) Detailed catalytic process of V_2O_5 nanozyme accelerating the oxidation of glutathione (GSH) in the presence of H_2O_2. Reprinted from ref. 12 with permission from Springer Nature, copyright 2014.
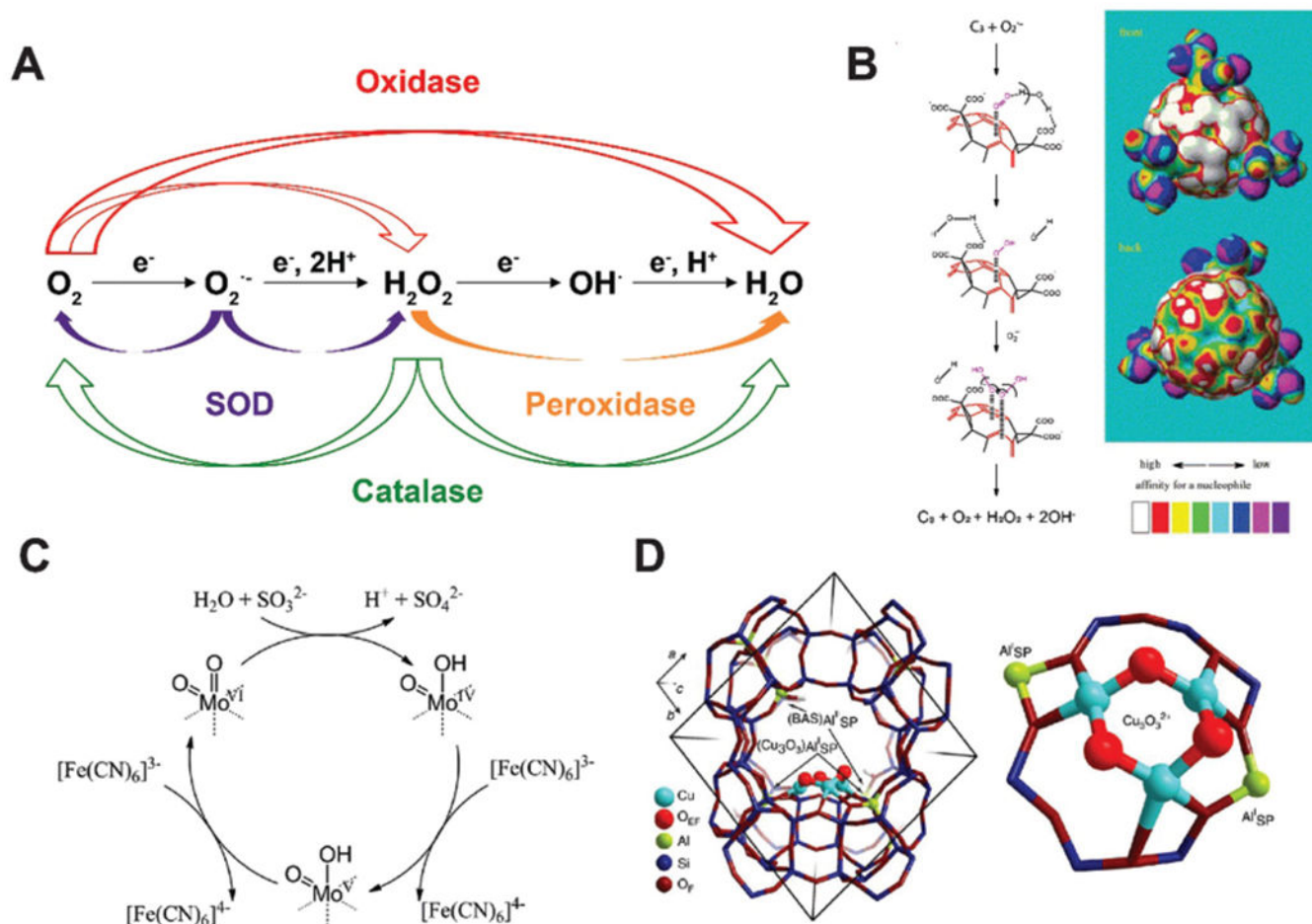
Fig. 3.
(A) Schematic of major reactions catalyzed by oxidase, superoxide dismutase (SOD), peroxidase and catalase. (B) Proposed SOD-mimicking mechanism (left) and the electron density mapping (right) showing the potential nucleophilic superdelocalizability of C_3-fullerene. Reprinted from ref. 16 with permission from Elsevier, copyright 2004. (C) Proposed sulfite oxidase-mimicking mechanism of MoO_3 nanozyme. Reprinted from ref. 18 with permission from American Chemical Society, copyright 2014. (D) Structural illustration of the active unit of Cu-containing MOF nanozyme for methane oxidation. Reprinted from ref. 19 with permission from Springer Nature, copyright 2015.
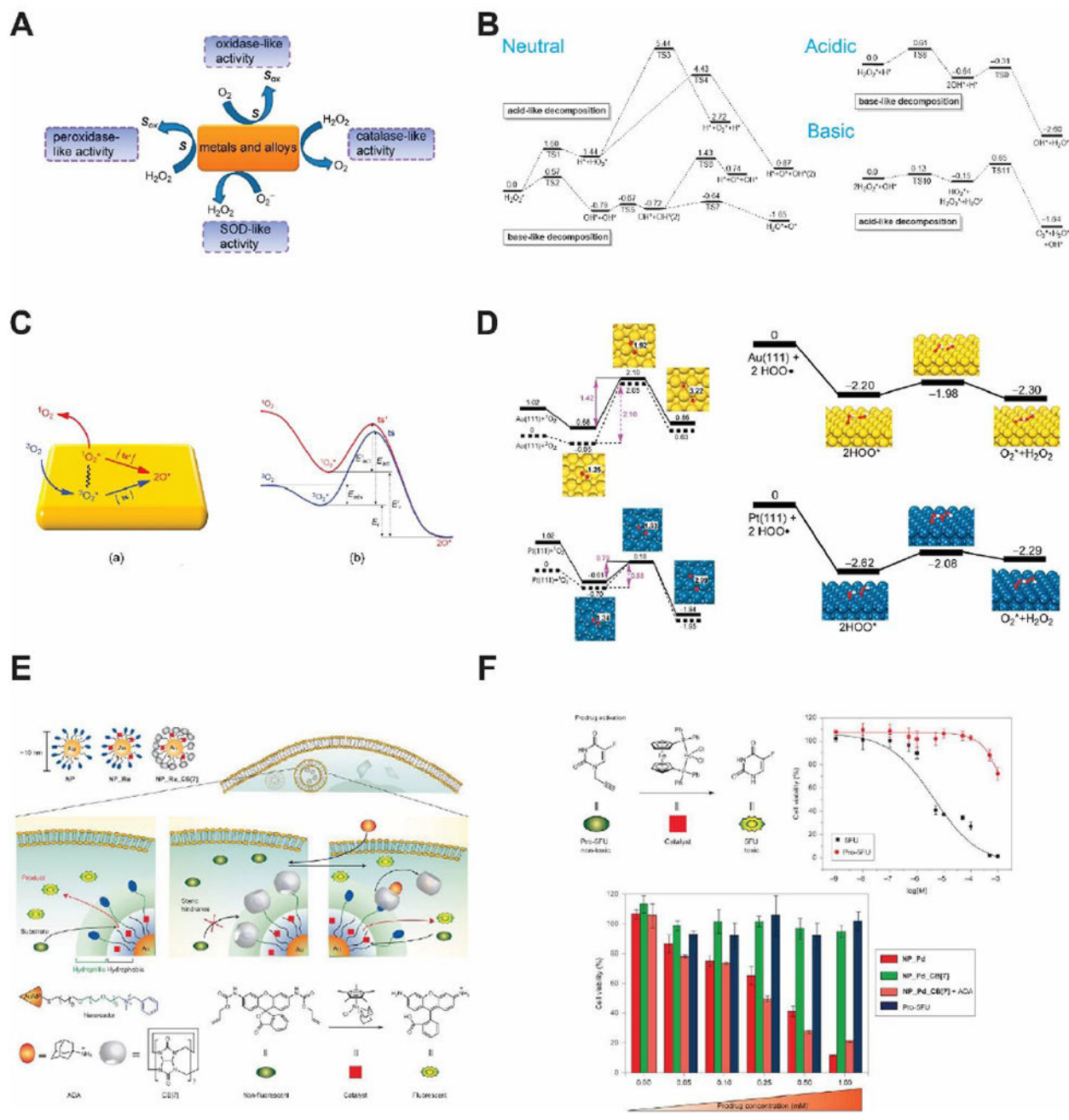
Fig. 4.

(A) Major redox reactions catalyzed by metal-based nanozyme systems and their alloys. Reprinted from ref. 23 with permission from American Chemical Society, copyright 2015. (B) Reaction energies for H_2O_2 decomposition on the surface of Au(111) nanozyme in different pH conditions (unit: eV). Reprinted from ref. 22 with permission from Elsevier, copyright 2015. (C) Schematic model showing the binding of $^3O_2$ on metal nanozyme surface and its activation routes. Reprinted from ref. 23 with permission from American Chemical Society, copyright 2015. (D) Reaction energies of O_2 and $O_2^{\bullet-}$ on the surface of

Au(111) and Pt(111) nanozymes for their oxidase and SOD-like activities (unit: eV). Modified from ref. 23 with permission from American Chemical Society, copyright 2015. (E) Schematic of transition metal (Ru and Pd) nanozymes catalyzing intracellular cross-coupling. Reprinted from ref. 25 with permission from Springer Nature, copyright 2015. (F) Prodrug activation in living cells regulated by transition metal nanozymes. Reprinted from ref. 25 with permission from Springer Nature, copyright 2015.
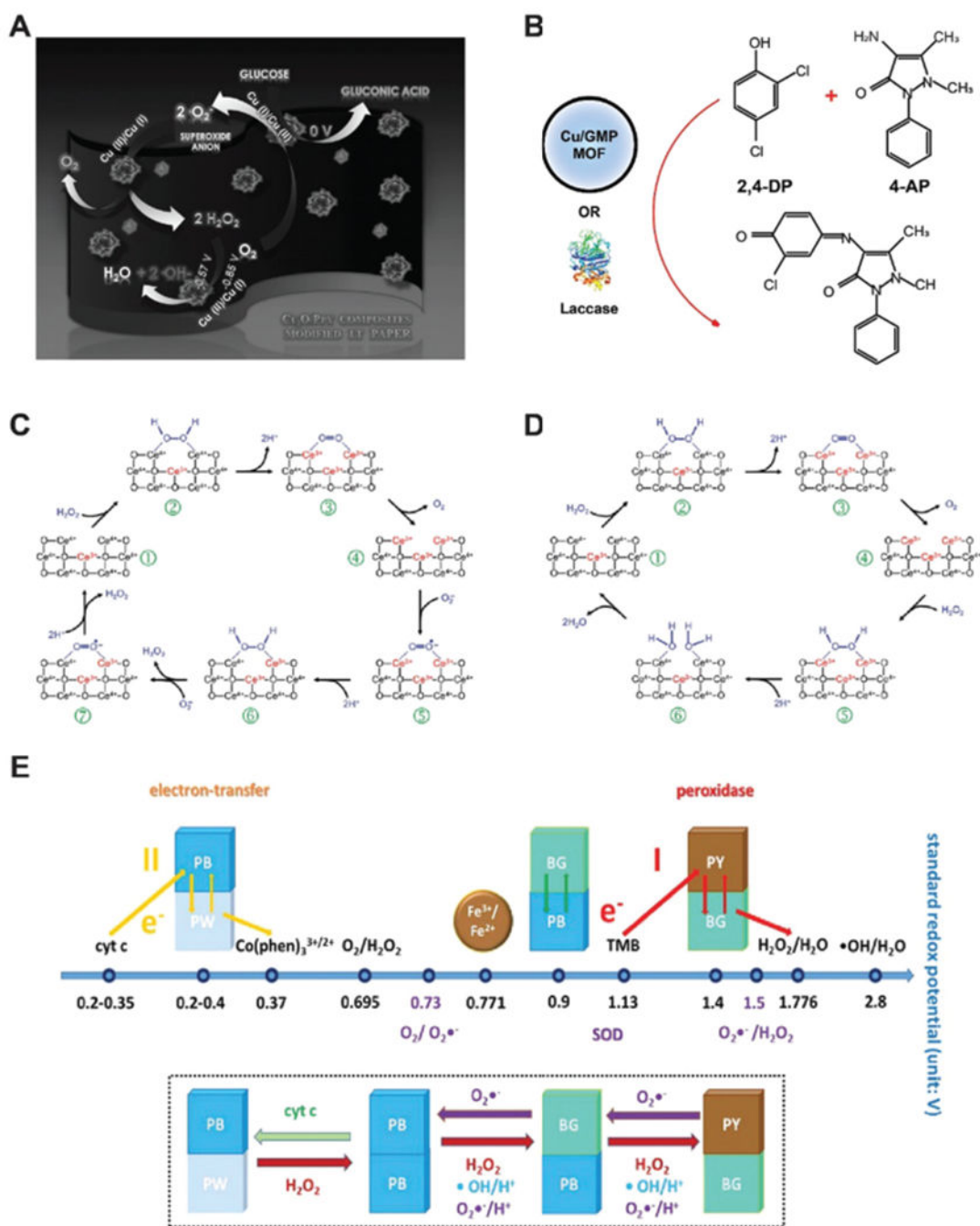
Fig. 5.
(A) Schematic of the glucose oxidase-like activity of Cu$_2$O@polypyrrole. Reprinted from ref. 26 with permission from Elsevier, copyright 2016. (B) Laccase-mimicking Cu$_2$O nanozyme catalyze the oxidation and coupling of phenols. Modified from ref. 28 with permission from American Chemical Society, copyright 2017. (C) Reaction mechanism of peroxidase and SOD-mimicking ceria nanozyme. Reprinted from ref. 29 with permission from the Royal Society of Chemistry, copyright 2011. (D) Illustration of catalase-mimicking ceria nanozyme. The flip-flops between Ce^{3+}/Ce^{4+} dictate the enzyme-mimicking behaviors

of ceria nanoparticle. Reprinted from ref. 29 with permission from the Royal Society of Chemistry, copyright 2011. (E) Prussian blue (PB) nanozyme presents peroxidase, catalase and SOD-like activities. The standard redox potentials of PB with different compounds are shown. Reprinted with permission from ref. 31 with permission from American Chemical Society, copyright 2016.
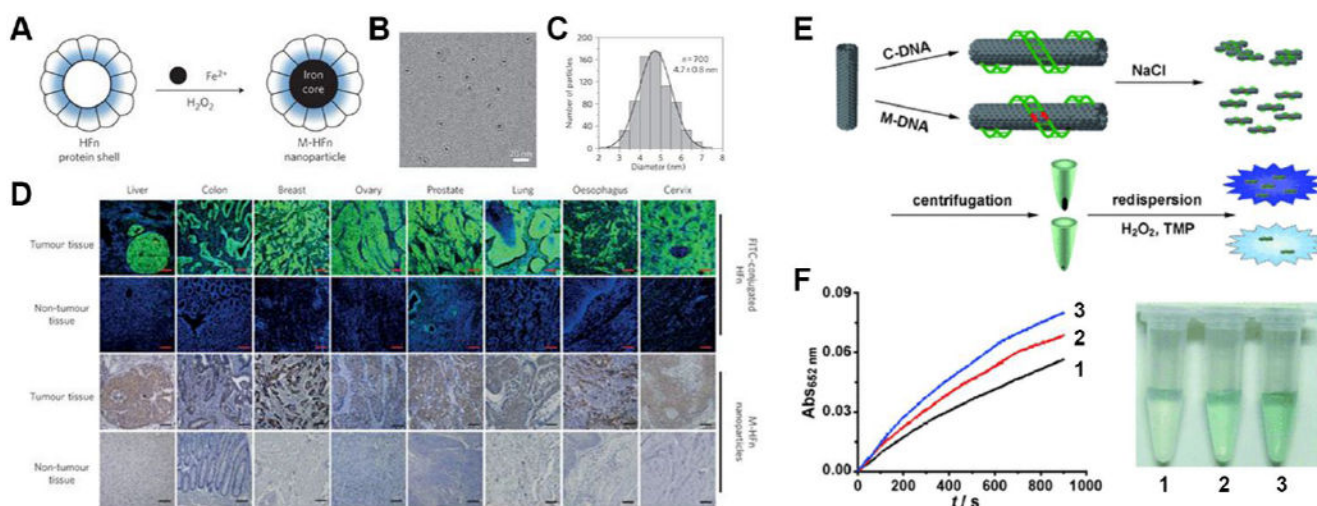
Fig. 6.

(A) Schematic of heavy-chain ferritin (HFn) coated magnetic Fe_3O_4 nanozyme (M-HFn). (B) cryoTEM image of M-HFn. (C) Size distribution of M-HFn. (D) M-HFn nanozyme distinguishes cancerous regions in clinical samples from normal tissues with high specificity. Reprinted from ref. 33 with permission from Springer Nature, copyright 2012. (E) Single-walled carbon nanotube (SWNT) differentiate complementary DNA (C-DNA) from mismatched DNA (M-DNA). Reprinted with permission from ref. 34. (F) Time-dependent UV absorbance curves (left) and photo images (right) of SWNT nanozymes without DNA (1), with M-DNA (2) and with C-DNA (3). Reprinted from ref. 34 with permission from John Wiley and Sons, copyright 2010.
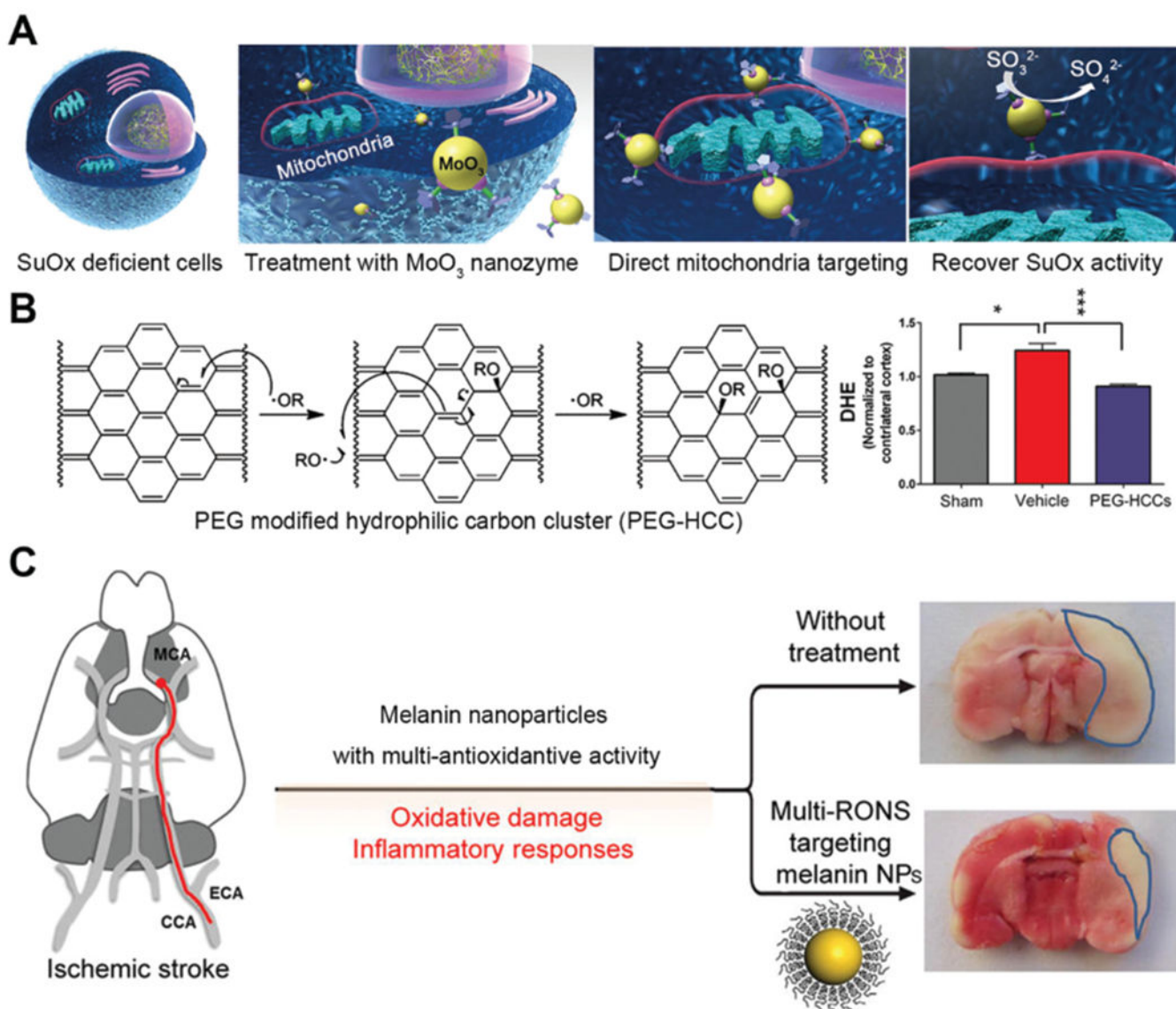
Fig. 7.
(A) Schematic of MoO_3 nanozyme serving as a sulfite oxidase (SuOx) mimic to treat cells with SuOx deficiency. Reprinted from ref. 18 with permission from American Chemical Society, copyright 2014. (B) PEG modified hydrophilic carbon cluster (PEG-HCC) acts as SOD to neutralize ROS (left) and prevent traumatic brain injury. Reprinted from ref. 35 with permission from American Chemical Society, copyright 2012. (C) Melanin nanoparticles fight ROS and protect rats from ischemic stroke after intracranial injection. Reprinted from ref. 32 with permission from American Chemical Society, copyright 2017.
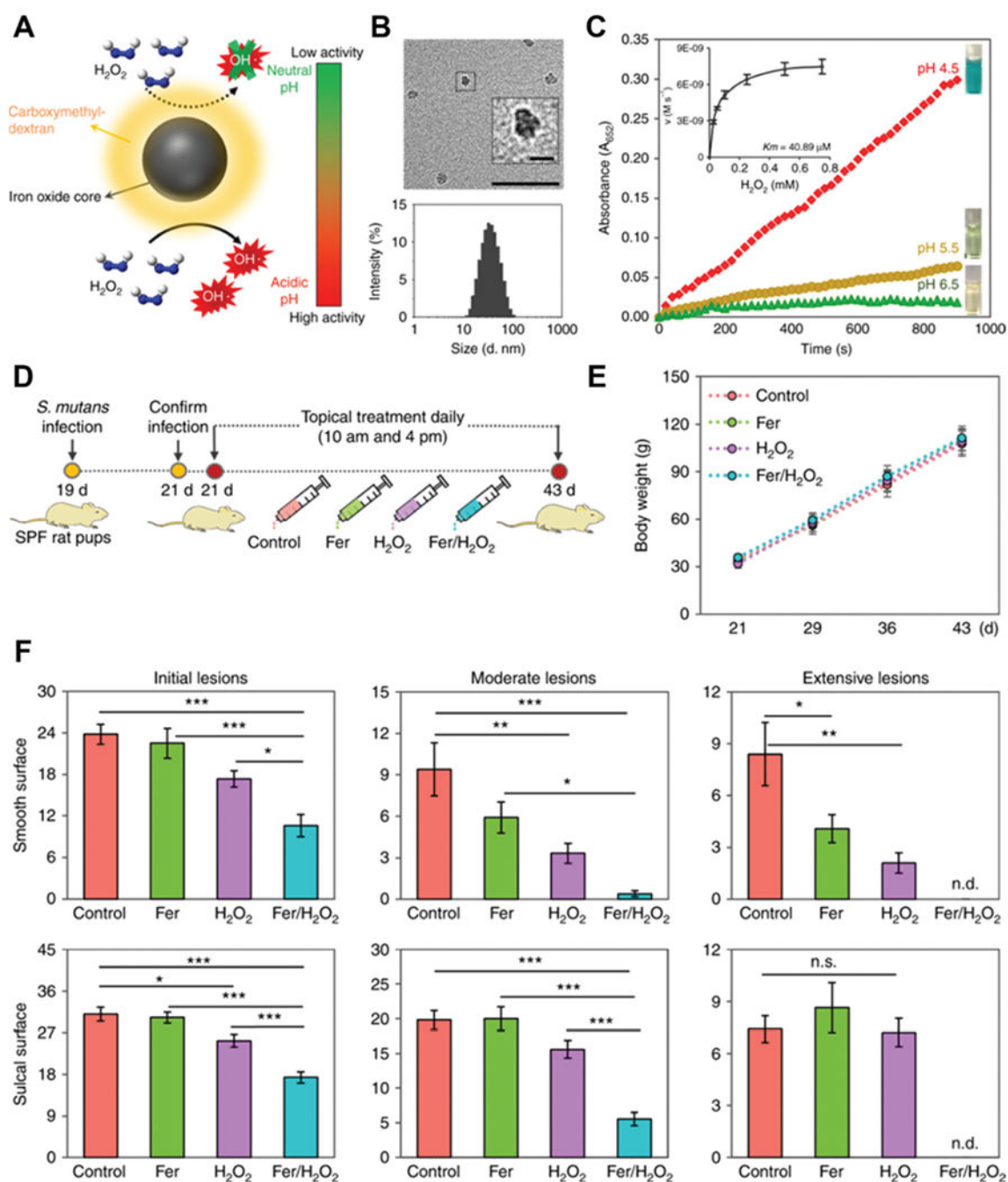
Fig. 8.
(A) Schematic of ferumoxytol nanozyme with pH-dependent peroxidase-mimicking activity. (B) TEM image (up) of ferumoxytol and its size distribution (down). Scale bar: 50 nm and 10 nm for the inset. (C) The peroxidase-like activity of ferumoxytol nanozyme at different pH. TMB was tested in the presence of H_2O_2 to yield a blue color. Inset shows the kinect profiling. (D) Time schedule of topical ferumoxytol/H_2O_2 treatment against a biofilm-associated oral disease (tooth decay) *in vivo*. (E) Body weight of tested animals did not change over time, suggesting the low toxicity of topical ferumoxytol/H_2O_2 treatment. (F)

Tooth decay (carries) onset and the severity of smooth and sulcal surfaces. Scoring of carries severity was recorded as stages and extent of carious lesion severity. This figure has been reprinted from ref. 37 with permission from Springer Nature, copyright 2018.
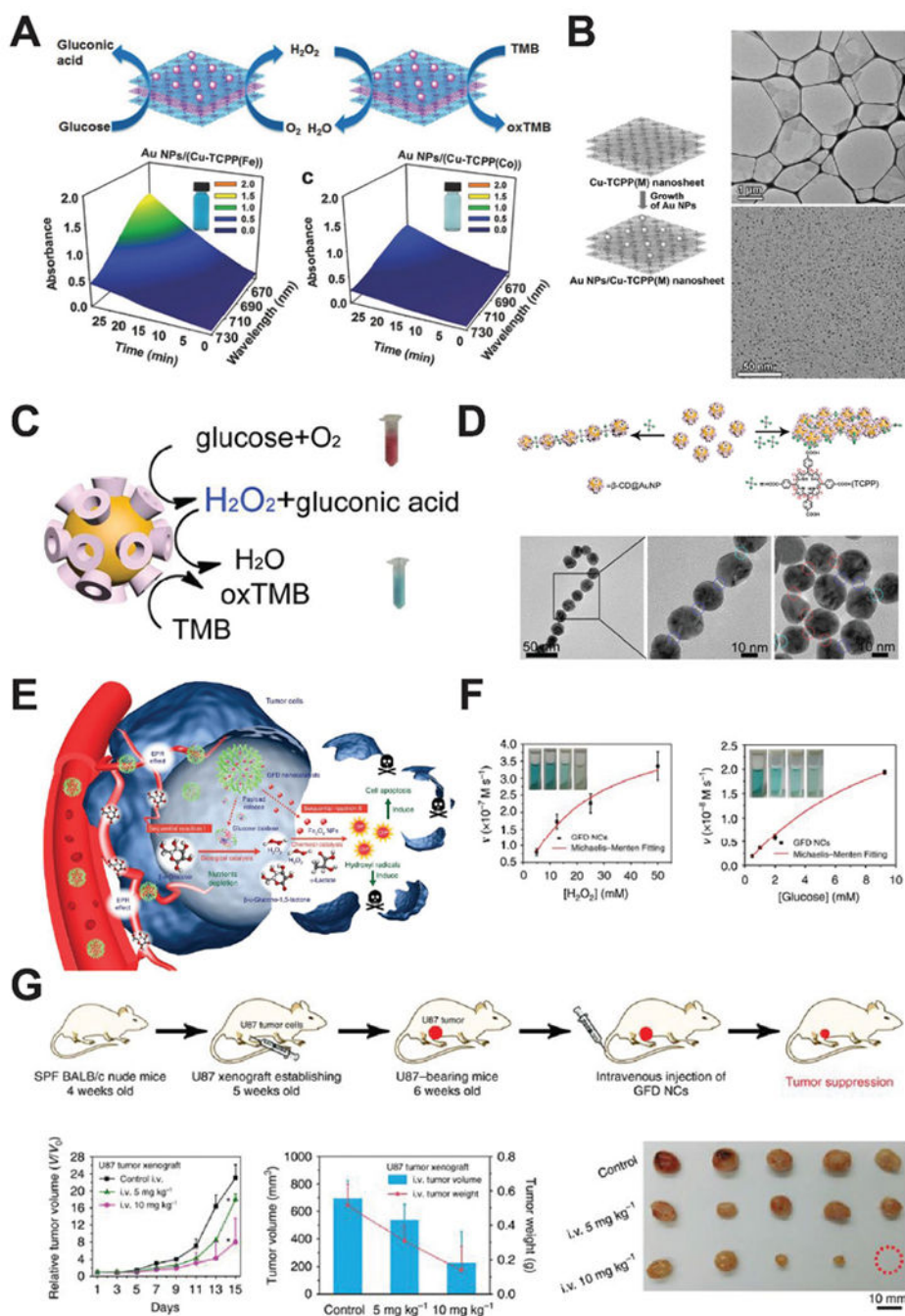
Fig. 9.
(A) Schematic of AuNP/Cu-TCPP(M) hybrid nanozyme catalyzing the oxidation of TMB for colorimetric detection of glucose, where M represents Fe and Co. Time-dependent absorption of the two nanozyme systems were shown on the bottom row. Reprinted from ref. 39 with permission from John Wiley and Sons, copyright 2017. (B) Synthesis process of AuNP/Cu-TCPP (left), and TEM images of the Cu-TCPP nanosheets (upper right) and AuNPs on the nanosheets. Reprinted from ref. 39 with permission from John Wiley and Sons, copyright 2017. (C) Schematic of the cascade reaction catalyzed by β-CD@AuNPs.

Reprinted from ref. 40 with permission from American Chemical Society, copyright 2016. (D) TCPP concentration dictates the assembly of β-CD@AuNPs *via* host–guest interactions. TEM images show the 1D and 2D self-assembly of CD@AuNP mediated by TCPP. Reprinted from ref. 40 with permission from American Chemical Society, copyright 2016. (E) Schematic of the GOx–Fe$_3$O$_4$ nanozyme system treating cancer after intravenous injection. Reprinted with permission from ref. 41. (F) Kinetic profiling of the GOx–Fe$_3$O$_4$ nanozyme against H$_2$O$_2$ and glucose. Reprinted from ref. 41 with permission from Springer Nature, copyright 2017. (G) Treatment schedule of tumor-bearing mice using GOx–Fe$_3$O$_4$ nanozyme. Tumor growth curve and representative images of tumors are shown. Reprinted from ref. 41 with permission from Springer Nature, copyright 2017.
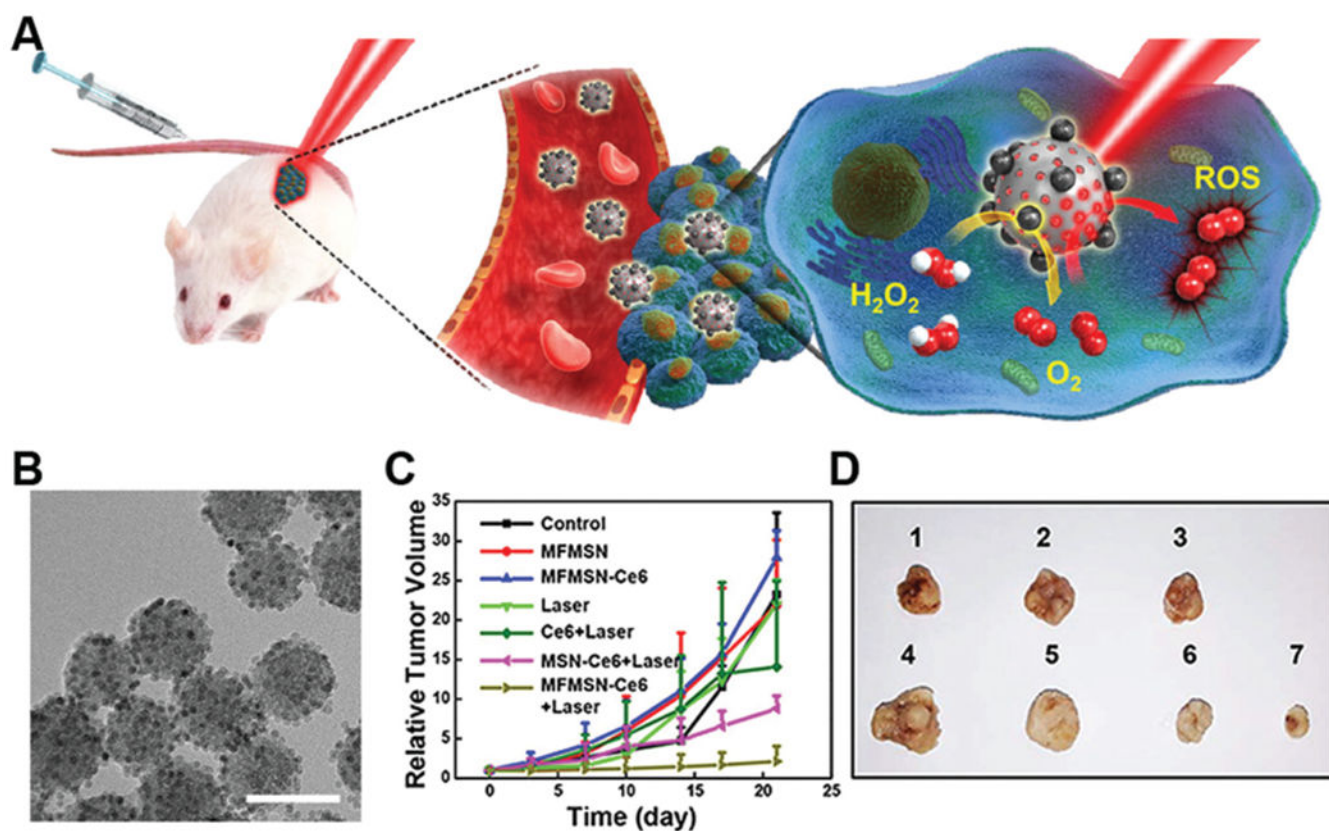
Fig. 10.
(A) Manganese ferrite nanoparticles (MFNs, $MnFe_2O_4$) combat hypoxia in tumor sites *via* self-acting catalase-mimicking activity. (B) The TEM image of MFNs shows that MFN of 6 nm size embedded on 50 nm silica nanoparticles. Scale bar 60 nm. Tumor growth curves (C) and representative tumor images (D) after administrating different treatments. MFN nanozymes with laser irradiation showed the optimal photodynamic therapy efficiency. Reprinted from ref. 42 with permission from American Chemical Society, copyright 2017.
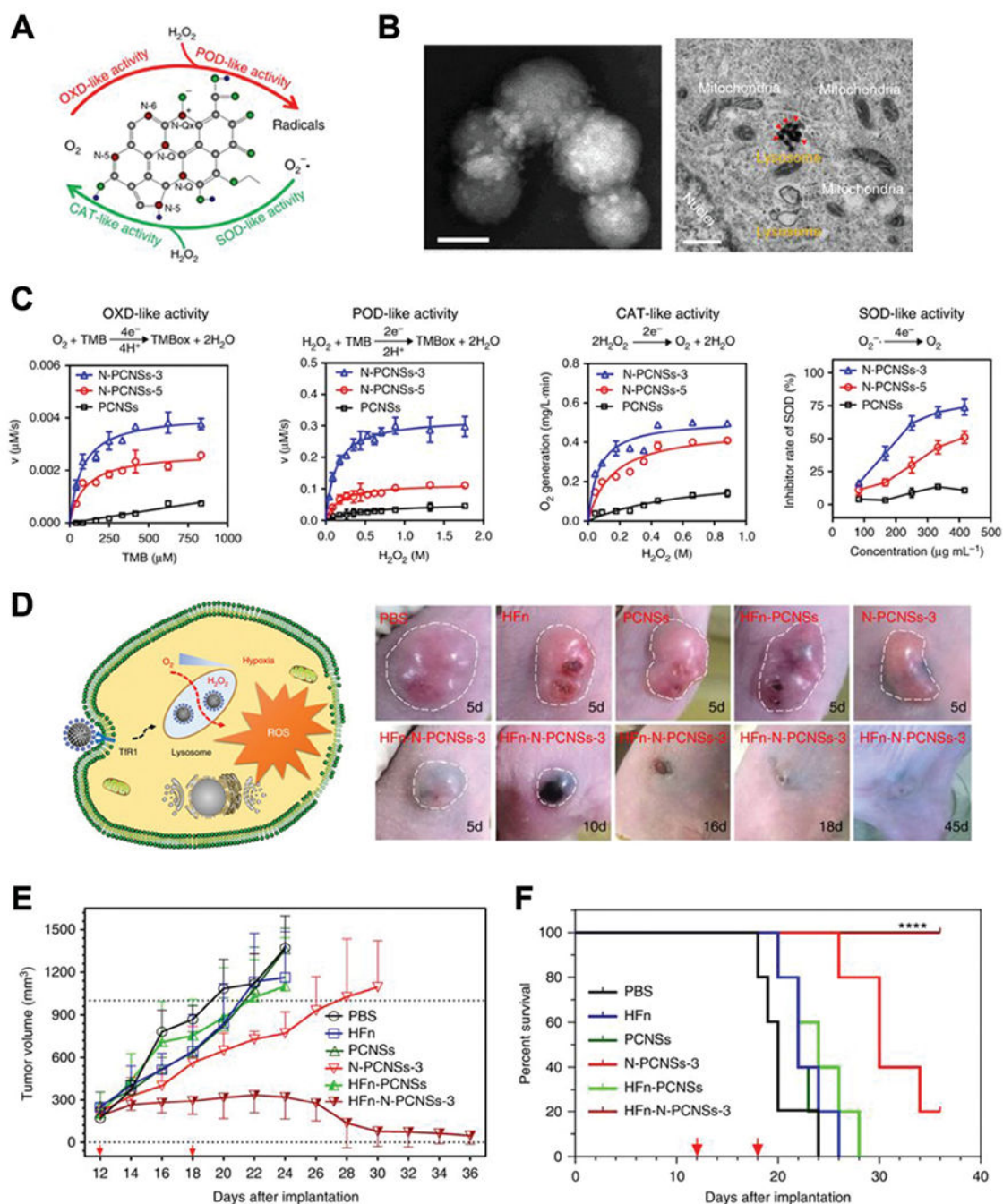
Fig. 11.

(A) Schematic of N-doped porous carbon nanozyme (N-PCNS) with multiple enzyme-like activities. (B) TEM image of HFn loaded N-doped porous carbon nanozyme (HFn-PCN, left, scale bar 50 nm) and cancer cells treated with HFn-PCN (right, scale bar 500 nm). (C) Kinetic profiles of N-PCNS mimicking oxidase, peroxidase, catalase and SOD. N-PCNS-3 has a higher nitrogen doping ratio than N-PCNS-5 and showed a higher enzymelike activities. (D) Schematic of HFn-PCN mediated tumor cell death and photo images of tumors treated with HFn-PCN in comparison with different control groups. Tumor growth

curves (E) and animal survival rates (F) after HFn-PCN treatment. Reprinted from ref. 43 with permission from Springer Nature, copyright 2018.
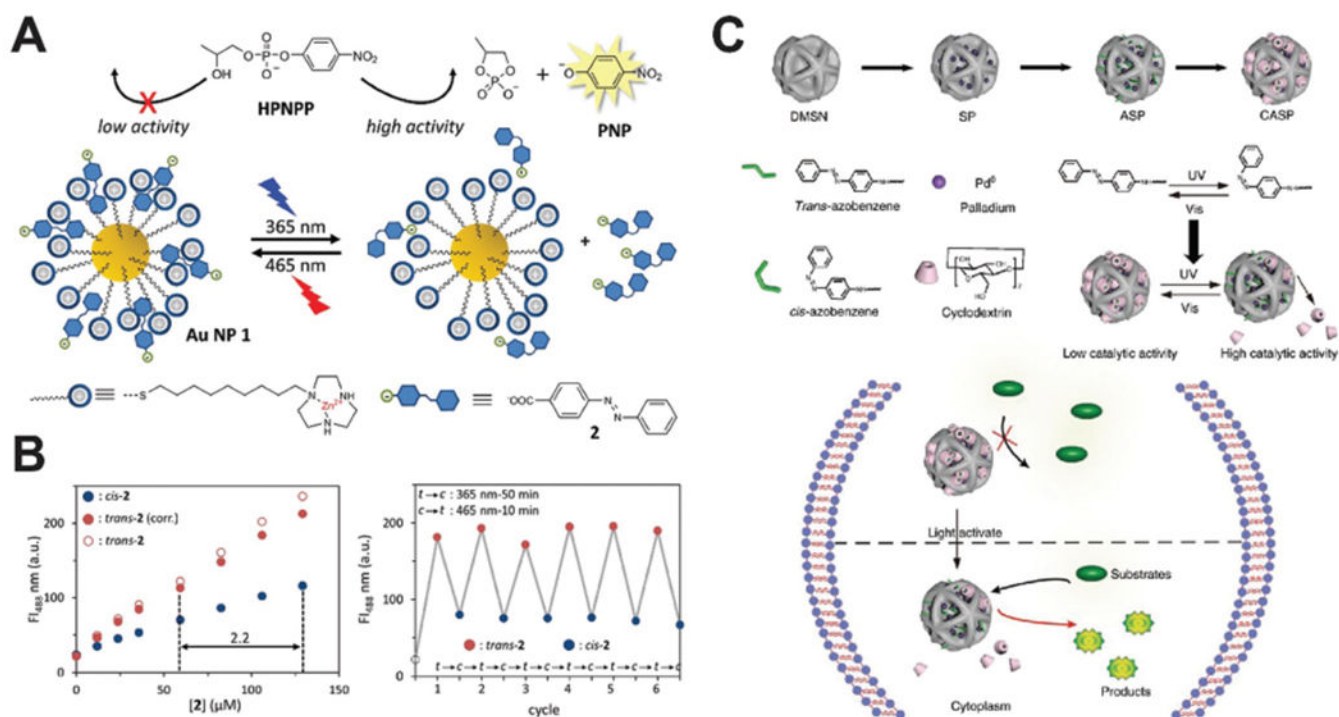
Fig. 12.
(A) Illustration of light-induced activation and deactivation of a AuNP nanozyme *via* the transformation of a small molecule co-factor. Reprinted from ref. 44 with permission from American Chemical Society, copyright 2017. (B) The fluorescent enhancement as a function of the co-factor concentration and the on/off light control of AuNP nanozyme showed consistency over multiple cycles. Reprinted from ref. 44 with permission from American Chemical Society, copyright 2017. (C) Schematic of the photo-responsive Pd^0 nanozyme for intracellular bioorthogonal reactions. The *trans-* and *cis-*form of azobenzene regulate the activity of nanozyme system. Reprinted from ref. 45 with permission from Springer Nature, copyright 2018.
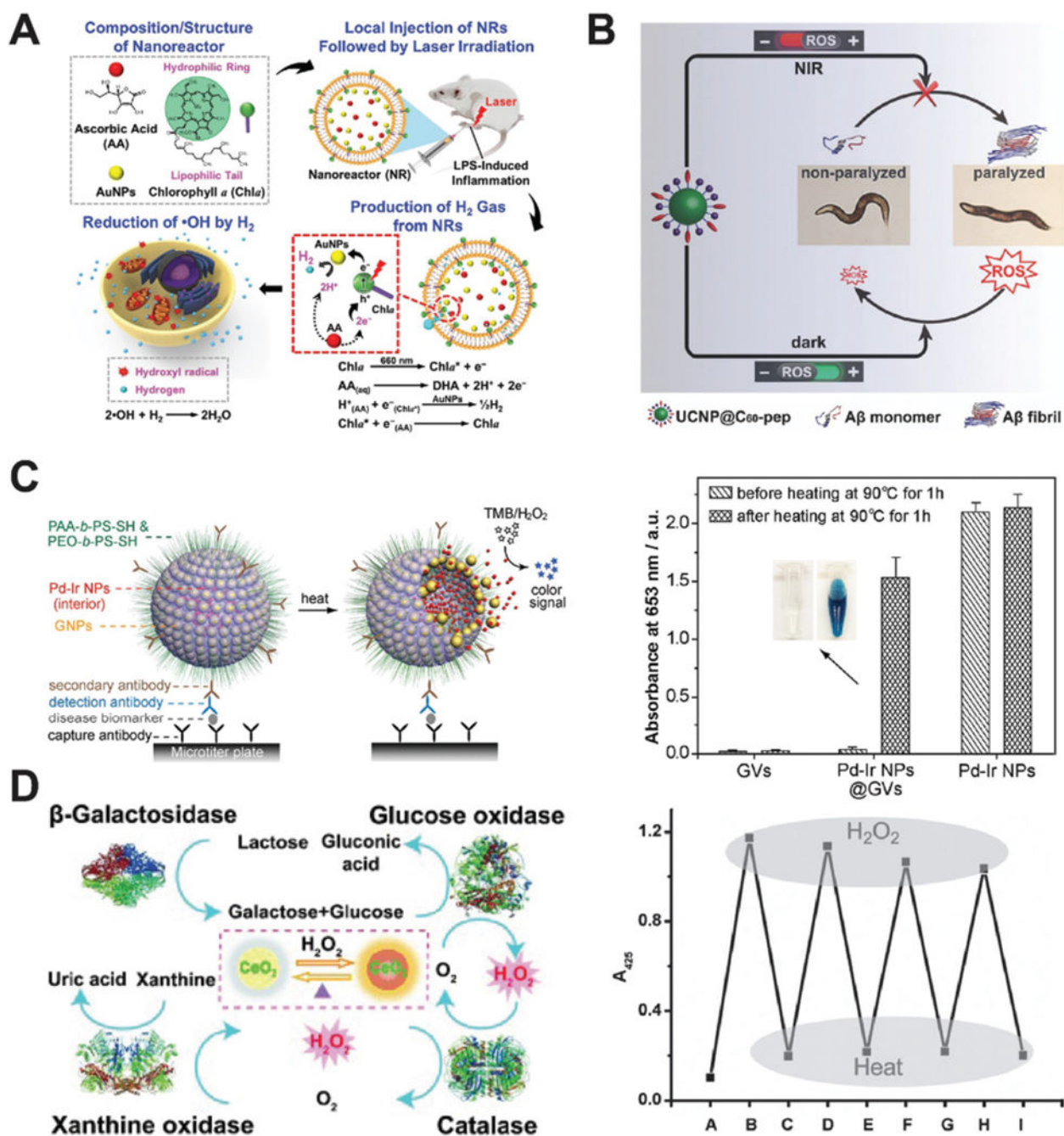
Fig. 13.

(A) Schematic of the preparation of light-induced hydrogenase-mimicking AuNP nanozyme system and photo-synthesis of H_2 to combat inflammation. Reprinted from ref. 46 with permission from American Chemical Society, copyright 2017. (B) Light-reversible ROS producing and scavenging properties of fullerene nanozyme to alleviate Alzheimer's Disease in a *Caenorhabditis eleans* model. Reprinted from ref. 47 with permission from John Wiley and Sons, copyright 2018. (C) Heat-activated Pd–Ir nanozyme system can be used for biomarker detection while non-heated one remains dormant as evidenced by colorimetric

analysis. Reprinted from ref. 48 with permission from American Chemical Society, copyright 2017. (D) Ceria nanozyme constitutes a logic gate system *via* the input of natural enzymes. The system can be regenerated by heat inactivation and present consistent color output. Reprinted from ref. 49 with permission from John Wiley and Sons, copyright 2012.
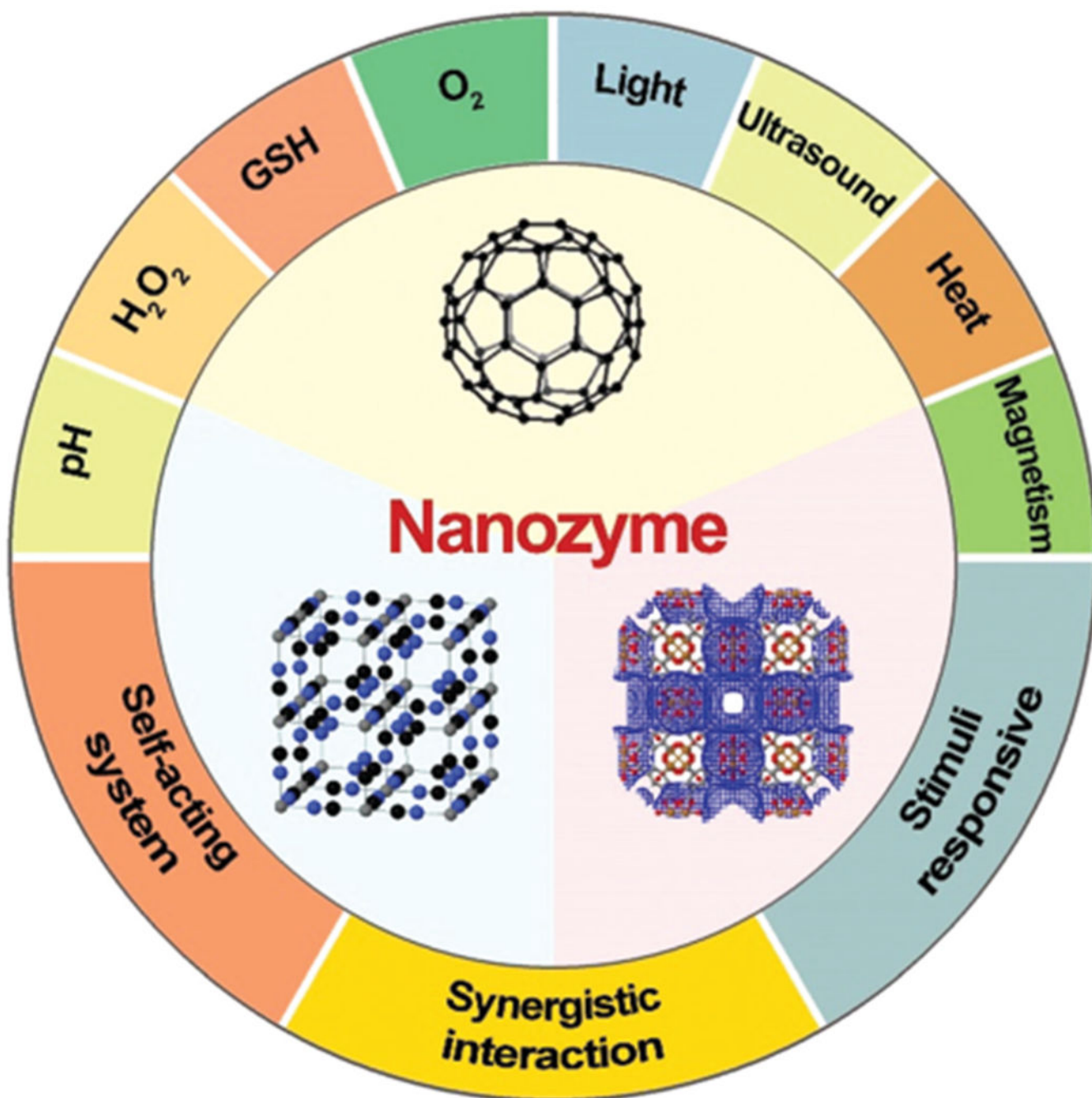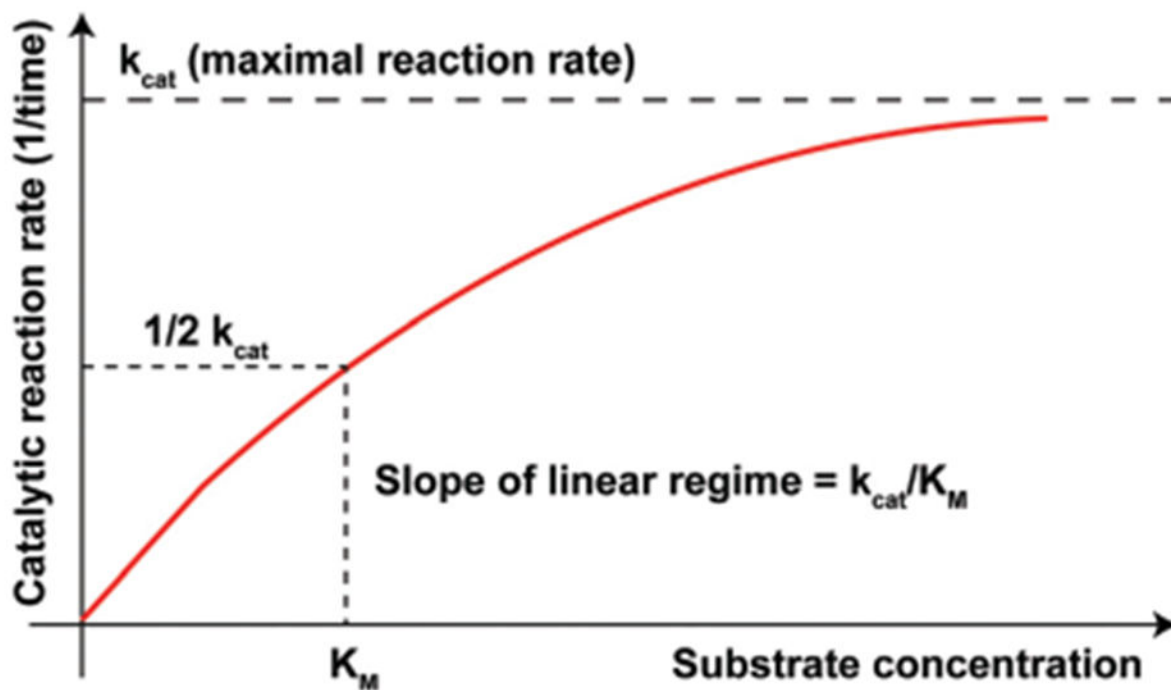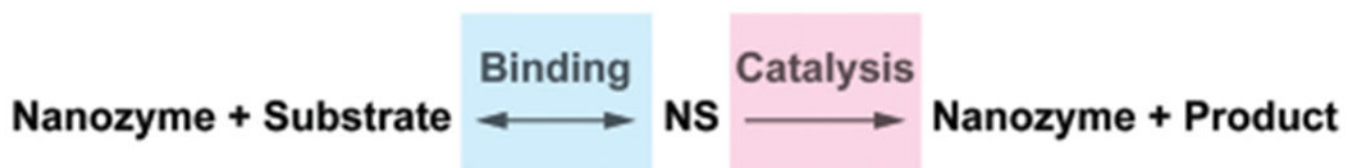
Scheme 1.
Nanozyme systems are engineered to be responsive to the biological microenvironment and external stimuli. Three nanostructures were generated on www.ChemTube3D.com.

Scheme 2.
A chemical reaction mechanism with nanozyme catalysis and a saturation curve for the nanozyme catalysis shows the relation between the substrate concentration and reaction rate, where k_{cat} and K_M can be defined from the curve.